NATIONAL ADVISORY COMMITTEE FOR AERONAUTICS

TECHNICAL NOTE 2751

A SIMPLE APPROXIMATE METHOD FOR CALCULATING SPANWISE LIFT DISTRIBUTIONS AND AERODYNAMIC INFLUENCE COEFFICIENTS AT SUBSONIC SPEEDS

By Franklin W. Diederich

Langley Aeronautical Laboratory
Langley Field, Va.

Washington
August 1952

NATIONAL ADVISORY COMMITTEE FOR AERONAUT

TECHNICAL NOTE 2751

A SIMPLE APPROXIMATE METHOD FOR CALCULATING SPANWISE LIFT DISTRIBUTIONS AND AERODYNAMIC INFLUENCE COEFFICIENTS AT SUBSONIC SPEEDS

By Franklin W. Diederich

SUMMARY

Several approximate methods for calculating lift distributions at subsonic speeds are combined and extended to form a simple step-by-step procedure for calculating symmetric and antisymmetric lift distributions for arbitrary angle-of-attack conditions on swept and unswept wings. Methods of estimating the required aerodynamic characteristics are included, but any available theoretical or experimental results may be used in several steps of the analysis to shorten the work and increase the accuracy. The extension of the method to the calculation of aerodynamic influence coefficients and of spanwise moment distributions is indicated.

INTRODUCTION

An empirical method (ref. 1) for calculating spanwise lift distributions on unswept wings has been used extensively in the past. In modified form (ref. 2) it has been applied to the calculation of spanwise lift distributions on swept wings. More recently, an improved method of calculating the lift distributions due to twist has been published (ref. 3).

In the present paper a limitation of the method of reference 3 as applied to antisymmetric twists is indicated and removed. The methods of references 1 to 3 are then combined with each other and with the results of another investigation (ref. 4) into a step-by-step procedure which starts with the lift-curve slope and the additional lift distribution and proceeds with the calculation of symmetric basic lift distributions, the lift distribution due to roll, the rolling-moment coefficient due to roll, and, finally, antisymmetric lift distributions. The

additional lift distribution is herein defined as the lift distribution for constant angle of attack across the span with a lift coefficient equal to 1. The basic lift distribution is defined as the lift distribution of a twisted wing at zero (total) lift. Means of calculating the aerodynamic characteristics required in the method are contained in this paper, but if any of these characteristics are known from other sources they may be incorporated in the procedure with a resultant saving in time and improvement of accuracy.

The method of this paper is derived in appendix A. It is outlined and some examples of its application to various plan forms and angle-of-attack conditions are presented and discussed in the body of the paper. Formulation of the method in matrix notation for the purpose of obtaining aerodynamic influence coefficients suitable for aeroelastic analyses is accomplished in appendix B of the present paper in the manner employed in reference 5. Inasmuch as the method of the present paper supersedes that of reference 2, on which reference 5 is based, appendix B of the present paper supersedes reference 5.

Means for estimating the spanwise distributions of pitching moments (or local centers of pressure) required in an aeroelastic analysis are indicated in appendix C.

SYMBOLS

A	aspect ratio, b^2/S
a	distance of local aerodynamic center from leading edge, fraction of chord
a_n	coefficient in Fourier series for γ
α	angle of attack, radians unless specified otherwise
$\bar{\alpha}$	average angle of attack, radians
α_e	effective angle of attack, radians
α_i	induced angle of attack, radians
α_δ	control-effectiveness parameter, $\frac{dc_l}{d\delta}\Big/\frac{dc_l}{d\alpha}$
b	wing span

b_n	coefficient in Fourier series for $\alpha \sin \theta$
$C_{1,2,3}$	coefficients for additional lift distribution
C_L	wing lift coefficient, Lift/qS
C_{L_α}	wing lift-curve slope, per radian unless specified otherwise
C_l	rolling-moment coefficient, Rolling moment/qSb
C_{l_d}	damping-in-roll coefficient, $-C_{l_p}$
C_{l_p}	rolling-moment coefficient due to rolling per unit helix angle (radians) at tip
c	chord, measured parallel to plane of symmetry
$\bar{c}$	average chord, S/b
c_l	section lift coefficient
c_{l_α}	section lift-curve slope, per radian unless specified otherwise
$c_{l_{\alpha_i}}$	section lift-curve slope in incompressible flow, per radian
cp_δ	distance from leading edge to center of pressure due to aileron deflection, fraction of chord
γ	loading coefficient, $cc_l/\bar{c}$
γ_a	loading coefficient for additional lift distribution
γ_b	loading coefficient for basic lift distribution
γ_d	loading coefficient for unit-rolling lift distribution
γ_r	loading coefficient for residual lift distribution
γ_1	loading coefficient for unit angle of attack
γ_2	loading coefficient for unit linear antisymmetric twist

δ control deflection in plane perpendicular to hinge line, radians

η section lift-curve-slope ratio, $c_{l_\alpha}/2\pi$

η^* dimensionless lateral distance from wing root, $\frac{\text{Lateral distance}}{\frac{b}{2} - \frac{w}{2}}$

F plan-form parameter, $A/\eta \cos \Lambda$

f additional-lift-distribution component due to sweep

I contribution of function f to rolling moment due to rolling, $4\int_0^1 fy^{*2}dy^*$

J abscissa of centroid of area of function f

K correction factor for effect of taper on lateral center of pressure in steady roll

k_0 finite-span correction for wing lift-curve slope, equation (7)

k_0' finite-span correction for wing lift-curve slope according to slender-wing theory

k_1 finite-span correction for basic lift distribution, equation (12)

k_2 finite-span correction for lift distribution in roll, equation (15)

k_3 finite-span correction for residual lift distribution, equation (22)

k_4 finite-span correction for rolling-moment coefficient due to roll, equation (17)

l section lift

Λ angle of sweepback at quarter-chord line

Λ_e	effective angle of sweepback in compressible flow, $\tan^{-1}\frac{\tan\Lambda}{\sqrt{1-M^2}}$
λ	taper ratio, Tip chord/Root chord
M	free-stream Mach number
Δp	pressure difference between upper and lower surfaces
q	dynamic pressure
S	wing area
t	wing thickness
w	width of fuselage
θ	trigonometric variable corresponding to y^*, $\cos^{-1}y^*$
y^*	dimensionless lateral ordinate, Lateral ordinate/Semispan
$\overline{y}^*$	dimensionless lateral ordinate of wing center of pressure
$\overline{y}_{L',p}$	effective lateral center-of-pressure location of resultant load causing rolling moment due to rolling

Subscripts:

II	two-dimensional flow
III	three-dimensional flow

DESCRIPTION OF THE METHOD

Symmetric Lift Distributions

The lift distribution for any symmetric angle-of-attack distribution may be considered to consist of two parts, a basic lift distribution with zero total lift and an additional lift distribution. The basic lift distribution for a given twist is defined as the distribution for the given wing with the angle of attack reduced equally at every point until the total lift is zero. The additional lift distribution is defined as the distribution which the wing would carry if it were untwisted and

the lift coefficient were equal to 1.0. If the additional and basic lift distributions are defined in terms of their loading coefficients, then

$$\left.\begin{aligned} \gamma_a &\equiv \left(\frac{cc_l}{\bar{c}}\right)_a = \frac{cc_l}{\bar{c}C_L} \\ \gamma_b &\equiv \left(\frac{cc_l}{\bar{c}}\right)_b \end{aligned}\right\} \qquad (1)$$

and the lift distribution for any variation of angle of attack or twist across the span may be written in the form

$$\gamma = C_{L_\alpha}\bar{\alpha}\gamma_a + \gamma_b \qquad (2)$$

This section is concerned with the determination of the quantities C_{L_α}, γ_a, $\bar{\alpha}$, and γ_b. If C_{L_α}, c_l, and γ_a are known they may, of course, be used instead of the values given herein.

Lift-curve slope.- The wing lift-curve slope may be obtained from the section lift-curve slope and a finite-span correction as

$$C_{L_\alpha} = c_{l_\alpha} \cos \Lambda \, k_0 \qquad (3)$$

where c_{l_α} and k_0 are determined as follows:

The section lift-curve slope is taken for the section perpendicular to the quarter-chord line at a Mach number equal to $M \cos \Lambda$; it may be estimated from the relation

$$c_{l_\alpha} = c_{l_{\alpha_i}} \frac{c_{l_\alpha}}{c_{l_{\alpha_i}}} \qquad (4)$$

where the ratio $\frac{c_{l_\alpha}}{c_{l_{\alpha_i}}}$ is given in figure 1 from the average of the theoretical data of reference 6 for airfoils of the NACA 63A, 64A, and 65A as well as the 63, 64, 65, and 66 (with subscripts) series as a function of the effective Mach number $M \cos \Lambda$ for several airfoil thickness ratios (perpendicular to the quarter-chord line). For all commonly used airfoil sections the lift-curve slope in incompressible flow $c_{l_{\alpha_i}}$ is known or may be calculated.

From the value of c_{l_α} a ratio

$$\eta = \frac{c_{l_\alpha}}{2\pi} \tag{5}$$

may be calculated and, hence, a plan-form parameter, defined in reference 4 as

$$F = \frac{A}{\eta \cos \Lambda} \tag{6}$$

According to reference 4, the value of k_0 may then be given in terms of this plan-form parameter as

$$k_0 = \frac{F}{F\sqrt{1 + \frac{4}{F^2}} + 2} \tag{7}$$

The factor k_0 is plotted in figure 2 as a function of the plan-form parameter F. For very large angles of sweepback another factor k_0', also shown in figure 2, should be used instead of k_0.

Additional lift distribution.- The additional lift distribution may be obtained from experimental data or theoretical calculations (ref. 7, for instance) or may be estimated from the relation derived in appendix A,

$$\gamma_a = C_1 \frac{c}{\bar{c}} + C_2 \frac{4}{\pi} \sqrt{1 - y^{*2}} + C_3 f \tag{8}$$

where the sweep-correction function f is given in figure 3 and where the coefficients C_1, C_2, and C_3 are given in figure 4. The function f depends on an effective angle of sweepback Λ_e defined by

$$\Lambda_e = \tan^{-1} \frac{\tan \Lambda}{\sqrt{1 - M^2}}$$

The elliptic distribution $\frac{4}{\pi}\sqrt{1 - y^{*2}}$ is also shown in figure 3 as the value of the function f for $\Lambda_e = 0$.

Unlike the value of γ_a given in reference 2, that given by equation (8) reduces to the correct value (that given by low-aspect-ratio theory or slender-wing theory) when the aspect ratio is very low and to the correct (strip-theory) value when the aspect ratio is very high. In general, equation (8) may be expected to apply to most practical plan forms with nearly straight quarter-chord lines, except those with very large effective angles of sweepback, say greater than about 60°. For such wings the lift distribution may be estimated from the results of slender-wing theory (refs. 8 and 9), as explained more fully in appendix A. According to slender-wing theory, the lift distribution is likely to be almost elliptic for a wing with a plan-form parameter less than about 2.5. A wing with a plan-form parameter greater than about 2.5 can be divided into three regions. In the two-dimensional region the lift distribution is proportional to the chord, in the tip region the lift drops off with infinite slope, and in the root region the lift drops to about $2/\pi$ of the value it would have if it were proportional to the chord. (See fig. 5.)

The lateral ordinate of the center of pressure $\bar{y}^*$ of the additional lift distribution or of any lift distribution for a constant angle of attack across the span is numerically equal to the moment about the origin of the function γ_a, since the area under the function γ_a is 1. Therefore,

$$\bar{y}^* = C_1 \frac{1 + 2\lambda}{3(1 + \lambda)} + C_2 \frac{4}{3\pi} + C_3 J \tag{9}$$

where J is the abscissa of the centroid of area of the function f and is given in figure 6 as a function of the effective angle of sweepback Λ_e. Equation (9) applies to a linearly tapered wing. For a wing which is not linearly tapered, the term $\frac{1 + 2\lambda}{3(1 + \lambda)}$ of equation (9) may be replaced by

$$\int_0^1 \frac{c}{\bar{c}}\, y^* dy^*$$

Basic lift distribution.- As described in appendix A, the basic lift distribution may be obtained from the lift-curve slope and the additional lift distribution as follows:

$$\gamma_b = k_1 C_{L_\alpha}(\alpha - \bar{\alpha})\gamma_a \tag{10}$$

where $\bar{\alpha}$ is evaluated from the integral

$$\bar{\alpha} = \int_0^1 \alpha\gamma_a \, dy^* \tag{11}$$

and the coefficient k_1 is obtained from the relation

$$k_1 = \frac{F\sqrt{1 + \frac{4}{F^2}} + 2}{F\sqrt{1 + \frac{36}{F^2}} + 6} \tag{12}$$

which is plotted in figure 2. The integration indicated in equation (11) may be performed graphically or numerically (by means of Simpson's rule, for instance).

If there are discontinuities in the angle-of-attack distribution, they should be faired before the angle-of-attack distribution is used in equations (10) and (11). Apparently the best results are obtained, on the average, when the fairing extends about 0.3 semispan on either side of the discontinuity and passes through the midpoint of the discontinuity; the faired curve should have the same area as the unfaired one.

Antisymmetric Lift Distributions

The lift distribution for any antisymmetric twist may be considered to consist of two parts: a rolling-type distribution, which is the distribution for the given wing with a linear antisymmetric twist of sufficient magnitude to have the same rolling moment as the twist distribution of interest, and a residual distribution, which is the difference between the rolling-type and the true distribution and which, by definition, has no rolling moment. If the unit-rolling type of distribution is defined by its loading coefficient

$$\gamma_d \equiv \frac{cc_l}{\bar{c}C_{l_d}}$$

where C_{l_d} is the rolling-moment coefficient of the distribution for a linear antisymmetric twist with unit angle at the tip (and is, hence, the negative of the conventionally defined rolling-moment coefficient due to rolling C_{l_p}), and if the residual distribution is defined by its loading coefficient

$$\gamma_r \equiv \left(\frac{cc_l}{\bar{c}}\right)_r$$

then any antisymmetric lift distribution may be written as

$$\gamma = C_{l_d}\alpha_e\gamma_d + \gamma_r \qquad (13)$$

where α_e is the tip angle required for a linear antisymmetric distribution with the same rolling moment as the distribution of interest. This section is concerned with the calculation of γ_d, C_{l_d}, α_e, and γ_r. If the values of γ_d and C_{l_d} are known they may, of course, be used instead of the values presented herein.

Unit-rolling distribution.- The lift distribution γ_2 for a linear antisymmetric twist with unit angle at the tip may be obtained from reference 10 or 11 or from the relation

$$\gamma_2 = k_2 C_{L_\alpha} y^* \gamma_a \tag{14}$$

where

$$k_2 = \frac{F\sqrt{1 + \frac{4}{F^2}} + 2}{F\sqrt{1 + \frac{16}{F^2}} + 4} \tag{15}$$

is derived in appendix A and shown in figure 2. The unit-rolling distribution γ_d is equal to γ_2 divided by the damping-in-roll coefficient C_{l_d}.

Damping-in-roll coefficient.- The damping-in-roll coefficient may be obtained from reference 10 or 11 or, as in reference 4, from the relation

$$C_{l_d} = \frac{K^2}{8} c_{l_\alpha} \cos \Lambda \, k_4 \tag{16}$$

where k_4 is a factor defined by

$$k_4 = \frac{F}{F\sqrt{1 + \frac{16}{F^2}} + 4} \tag{17}$$

which is plotted in figure 2. The factor K is a correction for taper effects on the lateral center of pressure introduced in reference 12 and is equal to twice the factor $\frac{\bar{y}_{L'_p}}{b/2}$ used in that paper. Another expression for C_{l_d} may be obtained from the method of the present paper:

$$C_{l_d} = \frac{1}{8} c_{l_\alpha} \cos \Lambda \, k_4 \left(\frac{2}{3} \frac{1 + 3\lambda}{1 + \lambda} C_1 + C_2 + IC_3 \right) \tag{18}$$

where C_1, C_2, and C_3 are the factors used in equation (8) and I is the moment of inertia of the function f defined as

$$I = 4 \int_0^1 f y^{*2} dy^* \tag{19}$$

The value of I is given in figure 6. If the wing does not have a linear taper the expression $4 \int_0^1 \frac{c}{\bar{c}} y^{*2} dy^*$ must be substituted for the term $\frac{2}{3} \frac{1 + 3\lambda}{1 + \lambda}$.

A comparison of equations (16) and (18) reveals that the factor K is equal to the expression $\sqrt{\frac{2}{3} \frac{1 + 3\lambda}{1 + \lambda} C_1 + C_2 + IC_3}$.

The two taper corrections K and $\frac{\bar{y}_{L'_p}}{b/2}$ are compared in figure 7(a) for unswept wings (since the correction $\frac{\bar{y}_{L'_p}}{b/2}$ does not apply to swept wings) and excellent agreement is seen to exist, except for plan-form parameters less than 6, for which the values of $\frac{\bar{y}_{L'_p}}{b/2}$ given in reference 12 are somewhat uncertain. Figure 7(b) shows the effect of sweep on the taper correction factor used in equation (18). This figure serves to explain the statement made in reference 12 that experimental evidence indicates that the effect of sweep on the factor $\frac{\bar{y}_{L'_p}}{b/2}$ is likely to be small, a statement which is difficult to reconcile with the great deviation of the additional lift distributions of swept (particularly sweptforward) wings from elliptical and also of their linear antisymmetric lift distributions from that of an elliptic wing. As may be seen from figure 7(b), however, the factor K, which is twice the factor $\frac{\bar{y}_{L'_p}}{b/2}$ and is obtained from spanwise lift distributions, is indeed substantially unaffected by sweep for angles of sweepback between 0° and about 35°, which are the ones for which most of the aforementioned experimental evidence was obtained; however, for sweptforward wings and for highly sweptback wings, sweep does have the expected effect on K.

Inasmuch as the correction of equation (18) permits sweep to be taken into account, whereas that of equation (16) does not, the use of equation (18) appears to be preferable for swept wings. For unswept wings both corrections give almost identical results.

Residual lift distribution.- The residual lift distribution may be obtained, as shown in appendix A, from the relation

$$\gamma_r = k_3 c_{l_d} \left(\frac{\alpha}{y^*} - \alpha_e \right) \gamma_d \qquad (20)$$

where the effective tip angle α_e is defined by

$$\left.\begin{aligned} \alpha_e &= \frac{1}{2}\int_0^1 \alpha\gamma_d \, dy^* \\ \text{or} \\ \alpha_e &= \frac{1}{2}\int_0^1 \frac{\alpha}{y^*}\,\gamma_d y^* dy^* \end{aligned}\right\} \tag{21}$$

and where the factor k_3 is defined by

$$k_3 = \frac{F\sqrt{1 + \frac{16}{F^2}} + 4}{F\sqrt{1 + \frac{64}{F^2}} + 8} \tag{22}$$

Any discontinuities in the angle-of-attack distribution must be faired before the distribution is used in equation (20) or (21). A convenient procedure for fairing this distribution is to plot the ratio α/y^* over the span and to fair it as suggested for discontinuous symmetric distributions. The faired distribution may then be used directly in the second form of equation (21).

ILLUSTRATIVE EXAMPLES

The method presented in the preceding sections has been applied to the calculation of lift distributions for a variety of plan forms in order to illustrate certain trends as well as to compare the results with those of other methods.

Additional lift distributions were calculated for six wings of different plan forms in incompressible flow. The results are shown in figure 8. The aspect ratios, angles of sweepback, taper ratios, and plan-form factors of these wings are given in table 1. In the calculation of the plan-form factors a section lift-curve slope of 2π was assumed. Also given in table 1 are the constants C_1, C_2, and C_3, which were taken from figure 4. The lift distributions calculated by the method of reference 13 (with 15 points on the span) and, in two cases, the lift distributions calculated by the method of reference 14 (with 126 lifting points on the span) are also shown in figure 8. There is good agreement between the approximate lift distributions given by the method of this paper and those calculated by the theoretical methods.

The lift-curve slopes and lateral centers of pressure of the additional lift distributions of the six wing plan forms considered in figure 8 are given in table 1, as calculated from equations (3) and (9) of the present paper and as calculated by the method of reference 13 (with 15 points on the span). The values of k_0 required in equation (3) for calculating C_{L_α} were obtained from figure 2 and are also included in table 1. Again, there is good agreement of the approximate values of C_{L_α} and $\bar{y}^*$ obtained by the method of this paper with the theoretical values.

Also calculated for plan forms 1 and 2 were basic lift distributions due to a unit parabolic twist and due to a unit deflection of a half-semispan flap $(\alpha_\delta \delta \cos \Lambda = 1)$. The results of these calculations are given in figures 9 and 10. For the parabolic twist $\alpha = y^{*2}$, equation (11) yields, in conjunction with the functions $\gamma_a \equiv \frac{cc_l}{\bar{c}C_L}$ taken from figure 8, a value of $\bar{\alpha}$. The function $\alpha - \bar{\alpha}$ is shown by the first curve in figures 9(a) and 10(a). The values of k_1 were taken from figure 2 and are 0.57 and 0.66 for plan forms 1 and 2, respectively. These values of $\bar{\alpha}$ and k_1, the approximate values of C_{L_α} given in table 1, and the additional lift distributions given in figure 8 were used in equation (10) to calculate the basic lift distributions $\gamma_b \equiv \left(\frac{cc_l}{\bar{c}}\right)_b$ (shown by the second curve in figs. 9(a) and 10(a)).

The basic distributions given by the second curve of figures 9(a) and 10(a) and the additional distributions given in figure 8 may be combined with the calculated values of $\bar{\alpha}$ and C_{L_α} to give the loading for the case where the wing has zero angle of attack at the root and is twisted parabolically so as to have a unit angle at the tip. This case is illustrated by the last curve of figures 9(a) and 10(a). These particular results are compared with the lift distributions which would be obtained from the method of reference 13. The agreement is better in this case for plan form 1 than for plan form 2.

For the effective twist due to flaps, the angle-of-attack distributions are shown in the first part of figures 9(b) and 10(b). The values of $\bar{\alpha}$ for the faired distribution were calculated from equation (11) and are 0.26 for plan form 1 and 0.27 for plan form 2. The curve $\alpha_{faired} - \bar{\alpha}$ was used in equation (10) to calculate the basic lift distributions (shown in the center part of figs. 9(b) and 10(b)) and the total lift distributions (shown in the right part of figs. 9(b) and 10(b)) as for the parabolic-twist case. The values of C_{L_α} and k_1

used to calculate the basic lift due to parabolic twist were also used in this case. The lift distribution calculated by the method of reference 13 with 15 points on the span (a correction for the discontinuity in the angle-of-attack distribution was included) is compared with the lift distribution calculated by the method of this paper. Again, better agreement of the approximate with the theoretical distribution is obtained for plan form 1 than for plan form 2.

In order to illustrate the treatment of antisymmetric angle-of-attack distributions, calculations have been made for plan form 2 of antisymmetric lift distributions due to a linear antisymmetric twist (damping in roll) and due to a unit deflection of half-semispan outboard ailerons $\left(\alpha_\delta \delta \cos \Lambda = 1\right)$. For the linear-twist case the distribution γ_2 was calculated from equation (14), with $k_2 = 0.80$ obtained from figure 2. The coefficient of damping in roll $C_{l_d} = 0.33$ was then calculated from equation (18), in which the values $k_4 = 0.63$ obtained from figure 2 and $I = 1.15$ obtained from figure 6 were used. The unit-rolling distribution was then obtained by dividing γ_2 by this value of C_{l_d}. The distribution is shown in figure 11(a). Also shown in figure 11(a) is the unit-rolling distribution calculated by the method of reference 13. The coefficient of damping in roll calculated by that method is $C_{l_d} = 0.38$. The unit-rolling distribution and the coefficient of damping in roll obtained by the approximate method of the present paper and by the theoretical method of reference 13 are in good agreement.

The function α/y^* for the aileron-type angle-of-attack distribution is shown at the top of figure 11(b); the fairing extends 0.3 semispan on either side of the discontinuity. The value of α_e was obtained from the second form of equation (21), with the approximately calculated function $\gamma_d \equiv \frac{cc_l}{\bar{c}C_{l_d}}$ given in figure 11(a), and is $\alpha_e = 1.12$. The value of k_3 was obtained from figure 2 and is $k_3 = 0.68$. With these values for k_3 and α_e, the function γ_d given in figure 11(a), the previously calculated value of C_{l_d}, and the faired function α/y^* given in figure 11(b), the residual lift distribution $\gamma_r \equiv \left(\frac{cc_l}{\bar{c}}\right)_r$ was calculated from equation (20) and is shown in the middle portion of figure 11(b). The lift distribution due to aileron deflection was then calculated from equation (13) and is shown in the bottom part of figure 11(b). Also given is the lift distribution calculated by the method of reference 13 with 15 points on the span and with a correction for the discontinuity in the angle of attack. The two lift distributions are in good agreement.

DISCUSSION

Inasmuch as experimental determination of pressure distributions is a very tedious process, complete information concerning the spanwise lift and moment distributions corresponding to all angle-of-attack conditions is rarely available. Hence, analytical methods for calculating these distributions are used almost universally in designing airplanes. Most of these methods are theoretical (for instance, for subsonic speeds see refs. 9 and 13 to 16). The reliability of these methods is well established; for wings without fuselage, nacelles, tip tanks, or external stores, they generally furnish very good approximations to the true distributions, provided the angle of attack, airfoil thickness, and Mach number are not too large. However, most of them are relatively time consuming. In order to overcome this deficiency, calculations for many plan forms have been made by some of these theoretical methods (refs. 7, 10, and 11, for instance), so that no further calculations need be made for the angle-of-attack conditions considered in these calculations. Another way of avoiding the tedious calculations required for the theoretical methods is to use empirical methods such as those of references 1 to 5, as well as that of the present paper, which consists in a combination of these methods.

Compared with the theoretical methods, an empirical method for calculating lift distributions has the disadvantage of being less accurate on the average, although the accuracy of the results of the empirical method is often adequate. Another disadvantage of empirical methods as compared with theoretical methods is the following: Once the accuracy of a theoretical method has been established by comparison with known results in a few cases, confidence can be placed in the results of this method for widely different cases. When an empirical method is used, the degree of confidence that can be placed in its results for cases widely different from those for which its accuracy has been established is not nearly so high. As far as the method of the present paper is concerned, this limitation implies that for the purpose of calculating lift-curve slopes and additional lift distributions the method is restricted to plan forms with nearly straight quarter-chord lines and effective angles of sweepback which are not greater than, say 60°. However, if these aerodynamic characteristics have been obtained experimentally or by means of accurate theoretical methods, other lift distributions and aerodynamic parameters can be calculated by this method for a much wider variety of plan forms by using the known lift-curve slope and additional lift distribution; also, the accuracy of the final results can be improved in this manner over that attainable by starting out with values of the lift-curve slope and additional lift distribution obtained by the method of this paper.

The matrix scheme of appendix B and the method for calculating the chordwise center of pressure given in appendix C make the method of this paper readily applicable to the aeroelastic analysis of reference 18.

For wings with straight quarter-chord lines, moderate angles of sweepback, and moderate aspect ratios the lift distributions calculated by the method of the present paper have been compared with those calculated by theoretical methods in connection with the illustrative examples. The agreement between the lift distributions and associated aerodynamic parameters calculated by the method of the present paper and those calculated by theoretical methods has been noted to be good. Inasmuch as the approximate method of this paper is based on lifting-line reasoning, and inasmuch as lifting-line theory is valid only for wings of high aspect ratio, a comparison of the results of the approximate method with results obtained by more rigorous theory for wings of very low aspect ratio may be of interest. The lift distributions for such wings can be obtained from reference 15, provided the wings do not have reentrant trailing edges.

For a wing of very low aspect ratio and with a parabolic twist $\alpha = y^{*2}$; thus $\gamma_a = \frac{\alpha}{\pi}\sqrt{1 - y^{*2}}$, $C_{L_\alpha} = \frac{\pi}{2} A$, and $k_1 = \frac{1}{3}$ (see fig. 2); also, $\bar{\alpha}$, as obtained from equation (11), is 1/4. Hence, from equations (10) and (2),

$$\gamma_b = \frac{2}{3} A\left(y^{*2} - \frac{1}{4}\right)\sqrt{1 - y^{*2}}$$

and

$$\gamma = \frac{A}{3}\left(2y^{*2} + 1\right)\sqrt{1 - y^{*2}}$$

$$= A\left(\frac{1}{2}\sin\theta + \frac{1}{6}\sin 3\theta\right)$$

(where $\cos\theta = y^*$), which is also the result given in table 1 of reference 15. That this perfect agreement of the two results is fortuitous may be seen from the fact that for a linear symmetric twist $\alpha = |y^*|$,

$$\gamma_b = \frac{2}{3}\left(y^* - \frac{4}{3\pi}\right)\sqrt{1 - y^{*2}}$$

and

$$\gamma = \frac{8}{3\pi} A\sqrt{1 - y^{*2}} + \frac{2}{3} A\left(y^* - \frac{4}{3\pi}\right)\sqrt{1 - y^{*2}}$$

$$= \frac{2}{3} A\left(y^* + \frac{8}{3\pi}\right)\sqrt{1 - y^{*2}}$$

whereas, according to reference 15,

$$\gamma = \frac{2A}{\pi}\left[\cos^2\theta \log \tan\left(\frac{\pi}{4} + \frac{\theta}{2}\right) + \sin\theta\right]$$

for this case. The two distributions are shown in figure 12(a) and are in good agreement.

The coefficient of damping in roll of a wing of very low aspect ratio can be obtained approximately from equation (18). From figure 2 and equation (17) the factor k_4 may be seen to be asymptotically equal to $F/8$ as F approaches 0; for $F = 0$ the factors C_1 and C_3 are 0 and the factor C_2 is 1 (see fig. 4), so that as a result of the definition of F,

$$C_{l_d} = \frac{\pi}{32} A$$

as given in reference 15. The factor $k_2 = 0.5$ for $F = 0$, so that

$$\gamma_2 = Ay^*\sqrt{1 - y^{*2}}$$

$$= \frac{A}{2} \sin 2\theta$$

as given in reference 15.

The unit-rolling distribution of a wing of very low aspect ratio is then

$$\gamma_d = \frac{\gamma_2}{c_{l_d}}$$

$$= \frac{32}{\pi} y^* \sqrt{1 - y^{*2}}$$

and the factor k_3 is 1/2. For a parabolic antisymmetric twist, $\alpha = y^{*2}$ on the right wing and $\alpha = -y^{*2}$ on the left wing. The effective tip angle is $\alpha_e = \frac{32}{15\pi}$, and the residual lift distribution on the right wing is

$$\gamma_r = \frac{A}{2}\left(y^{*2} - \frac{32}{15\pi} y^*\right)\sqrt{1 - y^{*2}}$$

so that the lift distribution on the right wing is

$$\gamma = A\left(\frac{1}{2} y^{*2} + \frac{16}{15\pi} y^*\right)\sqrt{1 - y^{*2}}$$

$$= A\left(\frac{1}{2} \sin\theta + \frac{8}{15\pi} \sin 2\theta + \frac{1}{8} \sin 3\theta\right)$$

whereas, according to reference 15,

$$\gamma = A\left[\frac{4}{3\pi} \cos^3\theta \log \tan\left(\frac{\pi}{4} + \frac{\theta}{2}\right) + \frac{2}{3\pi} \sin 2\theta\right]$$

for this case. These two distributions are shown in figure 12(b) and are in good agreement.

For the cubic antisymmetric twist $\alpha = y^{*3}$, the approximate method of the present paper happens to give the same result as reference 15:

$$\gamma = A\left(\frac{1}{4}\sin 2\theta + \frac{1}{16}\sin 4\theta\right)$$

In general, therefore, the method of the present paper gives results for wings of very low aspect ratio which are in excellent agreement with the results furnished by low-aspect-ratio theory.

The method of this paper has certain advantages over theoretical methods apart from the fact that the time required for an analysis by the empirical method is only a fraction of the time required for an analysis by means of one of the theoretical methods and is indeed comparable to the time required to obtain a desired lift distribution by interpolating between those furnished in references 7, 10, and 11. The method of the present paper is rather flexible, so that it may be used in some cases where present theoretical methods are inapplicable. For instance, in the case of a wing with a fuselage, nacelle, or tip tank, neither the method of this paper nor any generally available theoretical method can give the lift-curve slope or the additional lift distribution. However, if this information has been obtained experimentally, the method of this paper can give the lift distribution for any symmetric or antisymmetric twist with an accuracy sufficient for many purposes. (If the wing lift-curve slope is different from the lift-curve slope for the wing alone, the factors k_1, k_2, k_3, and k_4 can be obtained for the value of the plan-form parameter which corresponds to the given lift-curve slope rather than for the value of the true plan-form parameter.)

Another advantage of the empirical method over some theoretical methods is the ease with which it lends itself to the calculation of aerodynamic influence coefficients, which are required in an aeroelastic analysis. (See appendix B.) Also, for a wing in transonic flow the theoretical methods used with linearized-theory corrections for compressibility effects tend to give unsatisfactory results, as pointed out in reference 6. The empirical method of the present paper, however, is capable of furnishing useful results in certain cases of transonic flow because it is based on an interpretation of the three-dimensional Glauert-Prandtl rule which permits the use of known section characteristics and reconciles that rule with simple sweep theory. (See ref. 4.) For unswept wings of low aspect ratio and for sweptback wings which are slender in the sense of reference 9, that is, wings which have a small value of $A\sqrt{1 - M^2}$, equation 3 has been found to yield a good approximation to the observed values of the lift-curve slope in some instances

of transonic flow up to and beyond a Mach number of 1, provided the wings have thin sections and are at low angles of attack.

CONCLUDING REMARKS

A relatively simple method of calculating spanwise lift distributions for any angle-of-attack condition has been derived by combining and extending several previous theoretical methods. The method is such that the work can be shortened and the results improved at various stages of the computations by introducing experimental or theoretical values of certain aerodynamic parameters whenever they are available. In addition, the method lends itself readily to formulation of the load-distribution problem in terms of aerodynamic influence coefficients.

The results obtained by the present method compare favorably with those obtained by more time-consuming theories.

Langley Aeronautical Laboratory
National Advisory Committee for Aeronautics
Langley Field, Va., May 1, 1952

APPENDIX A

DERIVATION OF THE METHOD

Additional Lift Distribution

In the method of reference 1 the additional lift distribution γ_a for unswept wings is given by the average of the wing plan form and an ellipse of equal area, so that

$$\gamma_a = \frac{cc_l}{\bar{c}C_L} = \frac{1}{2}\left(\frac{c}{\bar{c}} + \frac{4}{\pi}\sqrt{1 - y^{*2}}\right) \tag{A1}$$

The corresponding relation for swept wings is given in reference 2 as

$$\gamma_a = \frac{1}{2}\left(\frac{c}{\bar{c}}\frac{m_o}{\bar{m}_o} + f\right) \tag{A2}$$

where m_o and $\bar{m}_o$ are, in the notation of reference 2, the section lift-curve slope and the average section lift-curve slope, respectively, and where f is a function of y^* which is different for each sweep. This function f fulfills a purpose similar to that of the function f used in the present paper but differs from it numerically.

That both of these relations are inapplicable to wings of either very high or very low aspect ratio may be seen from the fact that for very high aspect ratios the additional lift distribution is equal to the chord distribution $c/\bar{c}$, whereas for very low aspect ratios it is defined by the ellipse $\frac{4}{\pi}\sqrt{1 - y^{*2}}$ (see refs. 8 and 15), provided the wing does not have a reentrant trailing edge. Consequently, to cover the entire range of aspect ratios the equation for the additional lift distribution should have terms which involve the chord and the ellipse and a function which varies with sweep; the extent to which each of these three functions enters into the lift distribution should vary with aspect ratio. Consequently, the following relation suggests itself:

$$\gamma_a = C_1\frac{c}{\bar{c}} + C_2\frac{4}{\pi}\sqrt{1 - y^{*2}} + C_3 f \tag{A3}$$

where f is a new function which varies with sweep and is given in figure 3, and where the C's vary with aspect ratio in such a way that C_1 is 1 for infinite aspect ratio, C_2 is 1 for zero aspect ratio, and the sum of all three C's is always 1. A set of C's obtained by analyzing the results of the calculations by the method of reference 3 for a large variety of plan forms is presented in figure 4. The plan-form parameter $F = \frac{A}{\eta \cos \Lambda}$ (proposed in ref. 4) was chosen as the abscissa rather than the aspect ratio proper in order to take sweep and compressibility effects into account in a manner similar to that employed in reference 4 for the wing lift-curve slope.

In general, equation (A3) may be expected to apply to most practical plan forms with nearly straight quarter-chord lines, except those with very large effective angles of sweepback Λ_e, and to furnish more accurate results than do the approximate formulas of references 1 and 2, inasmuch as equation (A3), unlike those formulas, takes aspect ratio into account.

Wings with very large angles of sweepback can be analyzed by slender-wing theory. (See refs. 9 and 16.) The type of wings analyzed in reference 9 is characterized by a constant chord which is filleted generously at the trailing edge to the extent that the root chord is $\pi/2$ times the chord far away from the root. As may be deduced from reference 9, this wing can be divided into three regions in the manner indicated in figure 5. The pressure distribution in the part of the root region forward of the apex of the trailing edge is the same as it would be if the wing consisted of that part of the root region only, and therefore it can be obtained from the delta-wing theory (ref. 8). The spanwise lift distribution is constant and equal in magnitude to that in the two-dimensional region. In the two-dimensional region the chordwise pressure distribution is the same as in two-dimensional flow; the spanwise lift distribution is constant and is given by

$$l = qcc_{l_{\alpha_i}} \alpha \cot \Lambda$$

In the tip region the pressure is zero behind the leading edge of the tip chord, and the spanwise lift distribution drops off to zero in an approximately elliptic fashion. For an unfilleted wing the lift near the root must be less; if it is assumed to be proportional to the chord, the lift at the root is $2/\pi$ times the lift in the two-dimensional region.

As shown in reference 9, the lift-curve slope depends on the parameter $A/\cot \Lambda$, which for large angles of sweep is approximately equal

to $A/\cos\Lambda$. This value, in turn, is approximately equal to the plan-form parameter F, because for a wing with a large angle of sweepback the flow in planes perpendicular to the leading edge is almost incompressible at all subsonic speeds, so that the section lift-curve slope is approximately 2π. The variation of C_{L_α} with $A/\cot\Lambda$ given in figure 7 of reference 9 is therefore reproduced in figure 2 of the present paper as a variation of k_0' with F, where k_0' represents the ratio $C_{L_\alpha}/c_{l_\alpha}\cos\Lambda$ for slender plan forms.

Basic Lift Distribution

In reference 1 the basic lift distribution γ_b is given as one-half of the strip-theory value, or

$$\gamma_b = \frac{1}{2}c_{l_\alpha}(\alpha - \bar{\alpha})\frac{c}{\bar{c}} \tag{A4}$$

where

$$\bar{\alpha} = \int_0^1 \frac{c}{\bar{c}}\alpha\, dy^* \tag{A5}$$

In reference 2 the statement is made that the wing lift-curve slope C_{L_α} often gives better results in equation (A4) than the section lift-curve slope c_{l_α}, so that

$$\gamma_b = \frac{1}{2}C_{L_\alpha}(\alpha - \bar{\alpha})\frac{c}{\bar{c}} \tag{A6}$$

Both results were obtained on a purely empirical basis. Reference 17, however, indicates the possibility of a more rational approach, in that it proves by lifting-line theory that an average angle of attack $\bar{\alpha}$ defined by

$$\bar{\alpha} = \frac{C_L}{C_{L_\alpha}} \tag{A7}$$

can be obtained for any symmetric twist distribution from

$$\bar{\alpha} = \int_0^1 \alpha\gamma_a \, dy^* \tag{A8}$$

The reasoning behind this equation is somewhat as follows: According to lifting-line theory the lift distribution for any angle-of-attack distribution is given by the relation

$$\gamma = c_{l_\alpha} \frac{c}{\bar{c}}\left(\alpha - \alpha_i\right) \tag{A9}$$

and the distribution for a unit angle of attack across the span by

$$\gamma_1 = c_{l_\alpha} \frac{c}{\bar{c}}\left(1 - \alpha_{i_1}\right) \tag{A10}$$

where α_i and α_{i_1} are the induced angles of attack appropriate to the lift distributions γ and γ_1, respectively. These equations may be combined to yield

$$\gamma = \gamma_1\alpha + \left(\gamma\alpha_{i_1} - \gamma_1\alpha_i\right)$$

so that the lift coefficient for the given twist is

$$C_L = \int_0^1 \gamma \, dy^*$$

$$= \int_0^1 \gamma_1\alpha \, dy^* + \int_0^1 \left(\gamma\alpha_{i_1} - \gamma_1\alpha_i\right) dy^* \tag{A11}$$

The second integral may be shown to be zero by setting

$$\gamma = \sum_{1} a_n \sin n\theta$$

$$\gamma_1 = \sum_{1} a_{n_1} \sin n\theta$$

(where $\theta \equiv \cos^{-1} y^*$) so that, by lifting-line theory,

$$\alpha_i = \frac{1}{4A} \sum_{1} n a_n \frac{\sin n\theta}{\sin \theta}$$

$$\alpha_{i_1} = \frac{1}{4A} \sum_{1} n a_{n_1} \frac{\sin n\theta}{\sin \theta}$$

Then both the integral of $\gamma\alpha_{i_1}$ and that of $\gamma_1\alpha_i$ are equal to $\frac{\pi}{16A} \sum_{1} n a_n a_{n_1}$ for all symmetric angle-of-attack distributions, so that their difference is zero. Consequently,

$$C_L = \int_0^1 \gamma_1 \alpha \, dy^* \qquad \text{(A12)}$$

and since the additional lift distribution may be obtained by dividing γ_1 by its lift coefficient (which is C_{L_α}, since $\alpha = 1$ for the additional lift distribution) equation (A8) follows from equation (A12).

The preceding development suggests an equation for the basic lift distribution in the form of equation (A6), except that the factor $c/\bar{c}$ must be replaced with $cc_l/\bar{c}C_L$ in order that the total lift of the

basic lift distribution may be zero. Consequently, the basic lift distribution may be written as

$$\gamma_b = k_1 c C_{L_\alpha} (\alpha - \alpha_{L=0}) \sqrt{1 - y^2} \tag{A13}$$

where k_1 is a constant which depends on the plan-form parameter F and takes the place of the factor $1/2\pi$ in equation (A6).

The value of k_1 has been derived in reference 3 by means of series expansions. In the derivation of reference 3 it was required that the lifts and rolling moments of the lift distributions given by equation (A13) be equal to the values given by lifting-line theory. In the following paragraphs the same result is obtained in a slightly different manner which facilitates the extension of the method to antisymmetric lift distributions.

Inasmuch as the values of the lift-curve slope and damping in roll as given in references 4 and 12 are based on lifting-line results for elliptic wings, a reasonable value for k_1 should be obtainable through analysis of elliptic wings. For such wings, lifting-line theory predicts a lift distribution

$$\gamma = \sum \frac{\eta A}{A + 2n\eta} b_n \sin n\theta \tag{A14}$$

where $\eta \equiv \frac{c l_\alpha}{2\pi}$ and b_n is defined by

$$\alpha \sin\theta = \sum b_n \sin n\theta \tag{A15}$$

For a symmetric angle-of-attack distribution, only odd values of n are needed in equation (A14). The lift coefficient is then given by

$$C_L = \frac{\pi}{4} a_1 = 2\pi\eta \frac{A}{A + 2\eta} b_1 \tag{A16}$$

Since the lift is to be zero for the basic lift distribution, the first term of the series must be omitted, so that for the symmetric case the first term of the series is that for which $n = 3$. For the case of constant angle of attack, however, $b_1 = \alpha$ and all other b's are zero, so that

$$\gamma_1 = \frac{8\eta A}{A + 2\eta} \alpha \sin\theta \tag{A17}$$

$$C_{L_\alpha} = \frac{A}{A + 2\eta} c_{l_\alpha} \tag{A18}$$

and

$$\gamma_a = \frac{4}{\pi} \sin\theta \tag{A19}$$

Consequently, substituting equations (A15), (A18), and (A19) into equation (A13) gives

$$\gamma_b = k_1 \frac{A}{A + 2\eta} c_{l_\alpha} \frac{4}{\pi} \sum_{3} b_n \sin n\theta \tag{A20}$$

since $\bar{\alpha} = b_1$. This distribution should be the same as that given by equation (A14) (starting with the term $n = 3$). Clearly, no value of k_1 can satisfy this condition exactly. If the first terms in the two series are set equal, however, the others will not differ much; furthermore, since the first term is usually much larger than the others, the lift distributions will generally be almost identical if the first

terms of the series are equal. In order to satisfy that condition, k_1 must be taken as

$$k_1 = \frac{A + 2\eta}{A + 6\eta} \tag{A21}$$

which is identical to the result obtained in reference 3, except that there η was assumed to be 1.

A lifting-surface and sweep correction for k_1 may be deduced in the manner employed for the damping-in-roll coefficient in references 4 and 12. If the product $k_1 C_{l_\alpha}$ that occurs in equation (A13) is obtained from equations (A18) and (A21) and written in the form

$$k_1 C_{l_\alpha} = \frac{A/3}{\frac{A}{3} + 2\eta} c_{l_\alpha}$$

a correction identical to that for C_{l_α} but based on one-third the aspect ratio suggests itself. Consequently, upon introducing the sweep and lifting-surface corrections in this equation and dividing by C_{l_α}, the following relation is obtained:

$$k_1 = \frac{A\sqrt{1 + 4\left(\frac{\eta \cos \Lambda}{A}\right)^2} + 2\eta \cos \Lambda}{A\sqrt{1 + 36\left(\frac{\eta \cos \Lambda}{A}\right)^2} + 6\eta \cos \Lambda} \tag{A22}$$

This factor is plotted in figure 2 against the plan-form parameter $F \equiv \frac{A}{\eta \cos \Lambda}$.

Lift Distribution in Roll

If an equation similar to equation (A13) is applied to a linear antisymmetric angle-of-attack distribution with unit value at the tip ($\alpha = y^*$), the relation

$$\gamma_2 = k_2 C_{L_\alpha} y^* \gamma_a \tag{A23}$$

is obtained. A factor k_2 is used rather than k_1 because of the different nature of the induction effects for the symmetric and antisymmetric cases. The desired value of k_2 may be obtained from the lift distribution of elliptic wings, as follows:

For the angle-of-attack distribution in this case, equation (A15) yields $b_2 = \frac{1}{2}$, and all other b's are zero. Hence, equation (A14) yields

$$\gamma_2 = \frac{8\eta A}{A + 4\eta} \frac{1}{2} \sin 2\theta$$

whereas equation (A23) yields, after substitution of equations (A18) and (A19),

$$\gamma_2 = k_2 c_{l_\alpha} \frac{A}{A + 2\eta} \frac{4}{\pi} \sin \theta \cos \theta$$

The desired values of k_2 may be obtained by equating these two expressions for γ_2:

$$k_2 = \frac{A + 2\eta}{A + 4\eta} \tag{A24}$$

This value, also, is identical to that obtained in reference 3 for $\eta = 1$. It may be corrected for lifting-surface and sweep effects in the same manner as k_1, so that

$$k_2 = \frac{A\sqrt{1 + 4\left(\frac{\eta \cos \Lambda}{A}\right)^2} + 2\eta \cos \Lambda}{A\sqrt{1 + 16\left(\frac{\eta \cos \Lambda}{A}\right)^2} + 4\eta \cos \Lambda} \tag{A25}$$

This factor is also plotted in figure 2 against the plan-form parameter F.

Damping-in-Roll Coefficient

By calculating the rolling moment of the lift distribution given by equation (A23), a value for the damping-in-roll coefficient C_{l_d} $\left(= -C_{l_p}\right)$ may be obtained:

$$C_{l_d} = \frac{1}{2} c_{l_\alpha} \cos \Lambda \; k_2 k_0 \int_0^1 \gamma_a y^{*2} dy^* \tag{A26}$$

The product of the factors k_2 and k_0 is referred to as the factor k_4 in the following derivation.

If equation (A3) is substituted into equation (A26), the damping coefficient may be written as

$$C_{l_d} = \frac{1}{8} c_{l_\alpha} \cos \Lambda \; k_4 \left(\frac{2}{3} \frac{1 + 3\lambda}{1 + \lambda} C_1 + C_2 + IC_3 \right) \tag{A27}$$

where λ is the taper ratio, where I is defined by

$$I = 4 \int_0^1 f y^{*2} dy^* \tag{A28}$$

and is plotted in figure 6(b), and where the expression

$$4 \int_0^1 \frac{c}{\bar{c}} y^{*2} dy^*$$

must be substituted for the term $\frac{2}{3} \frac{1 + 3\lambda}{1 + \lambda}$ for wings which do not have linear taper. The value of C_{l_d} given by equation (A27) contains a correction for taper (the C_1 term) and a correction for the effect of sweep on the spanwise lift distribution (the C_3 term).

Antisymmetric Lift Distributions

Inasmuch as equation (A23) has been derived specifically for linear antisymmetric angle-of-attack distributions, it may not yield accurate results when applied to other antisymmetric angle-of-attack distributions, as is done in reference 3. The derivation of the equations for symmetric lift distributions in this appendix suggests a parallel derivation for antisymmetric distributions which has as its starting point not the relation given in reference 17, but rather its analog for antisymmetric lift distributions. The resulting equations for antisymmetric lift distributions are not as simple as equation (A23) - they imply a separation of the lift distribution into a damping-in-roll and a residual lift distribution analogous to the additional and basic lift distributions in the symmetric case - but they are applicable to a wider variety of antisymmetric angle-of-attack distributions than is the method of reference 3.

According to lifting-line theory applied to the linear antisymmetric case ($\alpha = y^*$),

$$\gamma_2 = c_{l_\alpha} \frac{c}{\bar{c}} \left(y^* - \alpha_{i_2} \right) \tag{A29}$$

where α_{i_2} is the induced angle of attack corresponding to the distribution γ_2. Combining this equation with equation (A9) for any arbitrary lift distribution yields the relation

$$\gamma y^* = \gamma_2 \alpha + \left(\gamma \alpha_{i_2} - \gamma_2 \alpha_i \right) \tag{A30}$$

The rolling-moment coefficient of any antisymmetric lift distribution γ may be written as

$$C_l = \frac{1}{2} \int_0^1 \gamma y^* dy^* \tag{A31}$$

so that, from equation (A30),

$$C_l = \frac{1}{2} \int_0^1 \gamma_2 \alpha \, dy^* + \frac{1}{2} \int_0^1 \left(\gamma \alpha_{i_2} - \gamma_2 \alpha_i \right) dy^*$$

By reasoning similar to that employed in connection with equation (A11) the second integral may be shown to be equal to zero for any antisymmetric γ distribution, so that

$$C_l = \frac{1}{2}\int_0^1 \gamma_2 \alpha \, dy^*$$

$$C_l = \frac{1}{2}\int_0^1 \frac{\alpha}{y^*} \gamma_2 y^* dy^* \tag{A32}$$

A damping-in-roll distribution γ_d for unit rolling-moment coefficient may be defined in a manner analogous to the additional lift distribution as

$$\gamma_d \equiv \frac{\gamma_2}{C_{l_d}}$$

since C_{l_d} is the rolling-moment coefficient of the γ_2 distribution. An effective angle of attack α_e, which is the angle of attack at the tip of a linear antisymmetric distribution with the same rolling moment as that of the given antisymmetric distribution γ, may then be defined as

$$\alpha_e = \frac{C_l}{C_{l_d}}$$

$$= \frac{1}{2}\int_0^1 \gamma_d \alpha \, dy^*$$

or

$$\alpha_e = \frac{1}{2}\int_0^1 \frac{\alpha}{y^*} \gamma_d y^* dy^* \tag{A33}$$

The analog of the basic lift distribution (which has zero lift) in the case of an antisymmetric distribution is the residual lift distribution γ_r, which has zero rolling moment. Equations (A13) and (A32) then suggest the form for this distribution:

$$\gamma_r = k_3 c_{l_d} \left(\frac{\alpha}{y^*} - \alpha_e \right) \gamma_d \tag{A34}$$

The rolling moment of γ_r is then zero, as required.

The factor k_3 may again be evaluated through an analysis of elliptic wings by lifting-line theory. For the antisymmetric case, only even values of n are contained in the series of equation (A14). Furthermore, since

$$c_l = \frac{\pi}{16} a_2 = \frac{\pi}{2} \eta \frac{A}{A + 4\eta} b_2 \tag{A35}$$

then for γ_r the term with $n = 2$ must be zero, and the series must begin with the term $n = 4$. But for an elliptic wing

$$c_{l_d} = \frac{1}{8} c_{l_\alpha} \frac{A}{A + 4\eta} \tag{A36}$$

$$\gamma_d = \frac{16}{\pi} \sin 2\theta \tag{A37}$$

and

$$\alpha_e = 2b_2$$

so that equation (A34) becomes

$$\gamma_r = k_3 \frac{1}{8} c_{l_\alpha} \frac{A}{A + 4\eta}\left(\frac{\alpha}{y^*} - 2b_2\right)\frac{16}{\pi} \sin 2\theta$$

or, as a result of equation (A15),

$$\gamma_r = k_3 \frac{1}{8} c_{l_\alpha} \frac{A}{A + 4\eta} \frac{32}{\pi} \sum_4 b_n \sin n\theta \tag{A38}$$

The values of γ_r given by equations (A38) and (A14) cannot be exactly equal for all antisymmetric angle-of-attack conditions, but if the first term of the series (which is usually much larger than all others) is made the same for both, the others will be approximately equal. Hence k_3 must have the value

$$k_3 = \frac{A + 4\eta}{A + 8\eta} \tag{A39}$$

which, by the same reasoning as that for k_1, may be corrected for lifting-surface, sweep, and compressibility effects by setting

$$k_3 = \frac{A\sqrt{1 + 16\left(\frac{\eta \cos \Lambda}{A}\right)^2} + 4\eta \cos \Lambda}{A\sqrt{1 + 64\left(\frac{\eta \cos \Lambda}{A}\right)^2} + 8\eta \cos \Lambda} \tag{A40}$$

This factor is plotted in figure 2 against the plan-form parameter F.

APPENDIX B

CALCULATION OF AERODYNAMIC INFLUENCE COEFFICIENTS

Aerodynamic influence coefficients are useful in methods of static aeroelastic analysis, particularly those employing matrices, such as that of reference 18. These influence coefficients may be considered to represent the lift (in dimensionless form) at one point of the span due to a unit angle of attack at another point. Such influence coefficients can be obtained by means of some of the theoretical methods by calculating the lift distributions corresponding to angle-of-attack distributions which are zero everywhere on the span except for one point, at which they are infinite in such a way that the area under the angle-of-attack distribution is zero. However, such lift distributions are difficult to calculate, and they may be obtained at points along the span which are inconvenient for an aeroelastic analysis.

The influence coefficients obtained by the procedure of reference 5 are based on the method of calculating spanwise lift distribution presented in reference 2. Individually these empirical coefficients do not have any significance, as do the coefficients described in the preceding paragraph, but when multiplied by the values of the angle of attack at several points on the span and summed, they do yield the lift at a point on the span in the same manner as the other influence coefficients. Apart from the fact that they can be calculated more simply and for any points on the span for which a set of integrating factors can be calculated, the empirical influence coefficients have the same advantages and disadvantages in comparison with the theoretical coefficients as do empirical methods in comparison with theoretical methods.

In this appendix a procedure is outlined for calculating influence coefficients in a manner which is similar to that employed in reference 5, but which is based on the method of calculating lift distributions given in the present paper rather than that of reference 2. In essence the procedure presented in this appendix consists in formulating this method of calculating lift distributions in matrix notation by using integrating matrices of the type presented in reference 18. Compared with influence coefficients calculated by the procedure of reference 5, the ones calculated by the procedure presented in this appendix have the advantages of greater accuracy and wider applicability, because the method of calculating spanwise lift distributions presented herein, on which the coefficients are based, has these advantages over earlier methods. The influence coefficients given by the procedure of reference 5 are applicable only to symmetric loadings and wings of moderate aspect ratio, whereas those given by the procedure of the present paper

are not subject to either of these restrictions. They should, therefore, be useful for most purposes for which aerodynamic influence coefficients are required.

The matrix notation used herein is the same as that used in reference 18.

Symmetric Case

Equations (2) and (10) may be combined to yield

$$\gamma = C_{L_\alpha}\left((1 - k_1)\bar{\alpha}\gamma_a + k_1\alpha\gamma_a\right)$$

or, in matrix notation,

$$\{\gamma\} = C_{L_\alpha}\left\{(1 - k_1)\lfloor\gamma_a\rceil\{\bar{\alpha}\} + k_1\lfloor\gamma_a\rceil\{\alpha\}\right\} \tag{B1}$$

where $\{\gamma\}$ is a column matrix which consists of the values of γ at several stations on the wing, $\{\alpha\}$ is a column matrix which consists of the values of α at those stations, $\{\bar{\alpha}\}$ is a column matrix of elements all equal to $\bar{\alpha}$, and $\lfloor\gamma_a\rceil$ is a diagonal matrix the nonzero elements of which are the values of γ_a at the same stations.

The integration indicated by equation (11) may be written in matrix form as

$$\bar{\alpha} = H\alpha_{root} + \frac{b - w}{b}\lfloor I_1\rceil\lfloor\gamma_a\rceil\{\alpha\} \tag{B2}$$

where H is defined by

$$H = \int_0^{w/b} \gamma_a \, dy^* \tag{B3}$$

and may be evaluated with sufficient accuracy for the present purpose from the relation

$$H = \frac{w}{6b}\left(\left(\gamma_a\right)_{y^*=0} + 4\left(\gamma_a\right)_{y^*=\frac{w}{2b}} + \left(\gamma_a\right)_{y^*=\frac{w}{b}}\right)$$

and where $\left[I_1\right]$ is an integrating matrix. As described in reference 18, a suitable integrating matrix may be obtained by approximating the integrand (the function $\alpha\gamma_a$) by parabolic segments. In view of the fact that γ_a goes to zero with infinite slope a special type of parabola has to be used, for instance, one which consists of a linear combination of the 1/2 power and 3/2 power of the distance from the tip. With this approximation to the curve of $\alpha\gamma_a$, the integrating matrix for stations at the wing root and every sixth of the distance from the wing root to the wing tip, for instance, may be written as

$$\left[I_1\right] = \underset{\text{Root}}{\left[0.05556,\ 0.20833,\ 0.15278,\ 0.16667,\ 0.14913,\ 0.22500,\ 0\right]}_{\text{Tip}} \quad \text{(B4)}$$

Equation (B2) can be written as

$$\bar{\alpha} = \overline{\left[I_1\right]\left[\gamma_a\right]}\{\alpha\}$$

where the row matrix $\overline{\left[I_1\right]\left[\gamma_a\right]}$ is obtained by calculating the row matrix $\frac{b - w}{b}\overline{\left[I_1\right]\left[\gamma_a\right]}$ and adding H to its first element. A square matrix $\overline{\left[I_1\right]\left[\gamma_a\right]}$ can then be constructed which consists of rows all equal to $\overline{\left[I_1\right]\left[\gamma_a\right]}$. With this square matrix, equations (B1) and (B2) can be combined and written as

$$\{\gamma_a\} = C_{L_\alpha}\left[\gamma_a\right]\left[\left(1 - k_1\right)\overline{\left[I_1\right]\left[\gamma_a\right]} + k_1\left[1\right]\right]\{\alpha\}$$

or

$$\{\gamma_a\} = c_{l_\alpha}[Q_s]\{\alpha\} \tag{B5}$$

where $[1]$ is the unit matrix, and where the matrix $[Q_s]$ defined by

$$[Q_s] \equiv [\gamma_a]\left[(1 - k_1)\overline{[I_1][\gamma_a]} + k_1[1]\right] \tag{B6}$$

is, in effect, an aerodynamic-influence-coefficient matrix for symmetric lift distributions.

In these matrices the values of γ, γ_a, and α are all taken at the same set of stations, and the integrating matrix must be set up for the same stations. Stations at the wing root and every sixth of the distance from the wing root to the wing tip (but excluding the wing tip proper, where γ_a is zero unless tip tanks or end plates are present) have been found convenient for many purposes. For these stations

$$\eta^* = 0,\ 0.1667,\ 0.3333,\ 0.5000,\ 0.6667,\ 0.8333$$

where η^* is the ratio of the lateral distance of the given station from the wing root to the length $\frac{b - w}{2}$. The integrating matrix given by equation (B4) may be used for these stations. The last element, 0, of the matrix of equation (B4) can be disregarded.

Antisymmetric Case

The antisymmetric lift distribution may be obtained from a combination of equations (13), (20), and (21) by use of matrix methods in the same manner as in the symmetric case. The result is

$$\{\gamma\} = c_{l_d}[\gamma_d]\left[\frac{1 - k_3}{2}\overline{[I_1][\gamma_d]} + k_3\left[\frac{1}{y^*}\right]\right]\{\alpha\} \tag{B7}$$

or

$$\{\gamma\} = c_{l_d}[Q_a]\{\alpha\} \tag{B8}$$

where

$$[Q_a] = \left[\gamma_d\right]\left[\frac{1 - k_3}{2}\overline{[I_1]\left[\gamma_d\right]} + k_3\left[\frac{1}{y^*}\right]\right] \tag{B9}$$

is an aerodynamic-influence-coefficient matrix for antisymmetric lift distributions. The matrix $\overline{[I_1]\left[\gamma_d\right]}$ is a square matrix with rows all equal to $\frac{w - b}{b}\left[I_1\right]\left[\gamma_d\right]$ and with a constant H' added to the first element. This constant is defined by

$$H' = \frac{1}{2}\frac{b}{w}\int_0^{w/b} y^*\gamma_d \, dy^*$$

and is given approximately by the relation

$$H' = \frac{w}{12b}\left(2\left(\gamma_d\right)_{y^* = \frac{w}{2b}} + \left(\gamma_d\right)_{y^* = \frac{w}{b}}\right)$$

The matrix $\left[\frac{1}{y^*}\right]$ can be calculated at the given stations from the relation

$$y^* = \frac{b - w}{b}\eta^* + \frac{w}{b}$$

APPENDIX C

MOMENT DISTRIBUTIONS

The spanwise distribution of the pitching moment is often of less interest than the lift distribution; for aircraft loads calculations the lift distribution usually is of primary interest, and for stability calculations the use of two-dimensional centers of pressure often yields sufficiently accurate over-all aerodynamic parameters. For some purposes, however, such as static aeroelastic calculations, a knowledge of the spanwise distribution of the pitching moment is important. In this appendix some available knowledge concerning this distribution is summarized for use in conjunction with the method of this paper.

The variation of the pitching moment along the span may be obtained from the lift distribution and the local centers of pressure. The local aerodynamic center, that is, the center of pressure due to angle of attack or twist of an uncambered wing, and the center of pressure due to control deflection are of most general interest.

Compared with the amount of information available on spanwise lift distributions, relatively little is known about the local centers of pressure of the lift distribution. The commonly used Weissinger method (ref. 13) for calculating lift distributions is characteristically incapable of furnishing local centers of pressure. Methods suitable for obtaining such information, such as Falkner's (ref. 14), are very cumbersome, and the local aerodynamic centers calculated by these methods are not altogether reliable. For instance, by using different vortex representations in Falkner's method different local aerodynamic centers are obtained, although the lift distributions are nearly the same. The centers of pressure due to aileron deflection cannot be calculated accurately by Falkner's method. An additional uncertainty in connection with the local centers of pressure is the fact that these centers are more sensitive than the lift distribution to deviations from the potential-flow conditions (as a result of boundary-layer separation, for instance) assumed in the analytical methods.

As a result of these considerations the information concerning local centers of pressure presented in subsequent sections should be regarded as qualitative rather than quantitative in nature; it is intended as a rough guide until more refined methods of calculating such information are available. The values of the local aerodynamic centers and centers of pressure due to control deflection are for incompressible flow. In order that subsonic compressibility effects may be taken into account approximately, the values should be estimated for an equivalent wing with an aspect ratio equal to $\sqrt{1 - M^2}$ times

the actual aspect ratio and with an effective sweep angle Λ_e, the tangent of which is $1/\sqrt{1 - M^2}$ times the tangent of the actual sweep angle Λ.

Local Aerodynamic Center

The local aerodynamic centers of an unswept wing of very high aspect ratio are at the quarter-chord line. As the aspect ratio decreases the local aerodynamic centers move forward, in particular near the tip of the wing. For constant-chord wings of vanishingly low aspect ratio, virtual-mass considerations indicate that the local centers of pressure are near the leading edge, although the applicability of low-aspect-ratio theory to such a wing may be questioned.

The local aerodynamic centers of several unswept constant-chord wings calculated by Falkner's method and those of two elliptic wings calculated from the results of reference 19 are shown in figure 13(a). At high and medium aspect ratios the wing taper has little effect on the local aerodynamic center, as may be seen, for instance, by comparing the results for the constant-chord and elliptic wings. At very low aspect ratios, on the other hand, virtual-mass considerations indicate that the effect of taper is likely to be more pronounced. If the leading edge is swept back, the local aerodynamic centers of a wing with vanishingly small aspect ratio may be estimated from the data shown for the low-aspect-ratio delta wing in figure 13(c) by considering the part of the wing enclosed by the leading edge and the line which connects the two ends of the leading edge to be a delta wing (see fig. 5). The aerodynamic-center locations shown in figure 14(a) were obtained in this manner.

The local aerodynamic centers of swept wings of very high aspect ratio are also on the quarter-chord line, except at the root and the tip. Near the wing root the local aerodynamic center, which is at the quarter-chord point for an unswept wing, moves back as the wing is swept back and approaches the midchord position for very high sweep angles; as the wing is swept forward the local aerodynamic center moves forward. At the wing tip, on the other hand, the local aerodynamic center moves forward toward the leading edge as the wing is swept back and rearward as the wing is swept forward.

The local aerodynamic centers for swept wings of medium aspect ratio depend both on the aspect ratio (in much the same way as for unswept wings) and on the angle of sweep (in a manner similar to that described in the preceding paragraph). The results of calculations by means of Falkner's method for constant-chord wings of various sweep angles and aspect ratios, as well as for one tapered wing and two delta

wings, are shown in figures 13(b) and 13(c). Comparison of the two plan forms of aspect ratio 2 with 60° sweepback corroborates the previously made statement that taper has an effect on the local aerodynamic center at low aspect ratios, although the effect is fairly small.

For wings of very low aspect ratio with sweptback leading edges and without reentrant trailing edges, the method of reference 8 may be used. In the case of delta wings it yields the aerodynamic-center variation along the span shown in figure 13(c).

For wings with angles of sweepback larger than about 60° the results of slender-wing theory presented in reference 9 may be used as a guide. The local aerodynamic-center positions obtained in this manner are shown in figure 5. These variations are only approximate, particularly in the case of the wings with small plan-form parameter, for which only the values at the root and tip are known.

The local-aerodynamic-center lines shown in figure 13 have been calculated for constant angles of attack along the span. From the data of reference 19, however, a local-aerodynamic-center line can be calculated for a linear antisymmetric angle-of-attack distribution of an elliptic wing of aspect ratio 6. This line agrees perfectly with the one shown in figure 13. Consequently, it may be assumed that the nature of the angle-of-attack distribution along the span has little effect on the local-aerodynamic-center location for unswept wings, and probably for swept wings as well.

Local Center of Pressure Due to Control Deflection

For unswept wings of high aspect ratio and, except at the root and the tips, for swept wings of high aspect ratio, the two-dimensional value of the center of pressure due to control deflection may be used. For medium aspect ratios no results comparable to those for the local aerodynamic center are available. In order that some indication of the probable location of the center of pressure relative to the two-dimensional value may be obtained, the difference between the lift actually carried at any section of the wing and that which would be carried if the section were in two-dimensional flow may be considered to act at the aerodynamic center. This assumption leads to the equation

$$\Delta c_{p_\delta} \equiv c_{p_{\delta_{III}}} - c_{p_{\delta_{II}}}$$

$$\approx \left(c_{p_{\delta_{II}}} - a\right) \frac{\gamma_{II} - \gamma_{III}}{\gamma_{III}}$$

where γ_{III} is the value of γ calculated by the method of this paper, a is the local aerodynamic center, and

$$\gamma_{II} = \frac{c}{\bar{c}} c_{l_\alpha} \alpha_\delta \cos \Lambda (\delta \cos \Lambda)$$

$$= \frac{c}{\bar{c}} c_{l_\delta} \delta \cos^2 \Lambda$$

where δ is the control deflection measured in a plane perpendicular to the hinge line and α_δ is the two-dimensional value of the control effectiveness.

For wings of very low aspect ratio the method of reference 8 may sometimes be used to calculate centers of pressure due to control deflection, provided both the wing and the control surface have sweptback leading edges, the trailing edge is not reentrant, and the hinge line is perpendicular to the free stream. The centers of pressure due to a symmetric control deflection as given by the apparent-mass concept on which reference 8 is based are shown in figure 14(b) for two such wings. When the entire tip of a low-aspect-ratio wing is rotated about a hinge line perpendicular to the free stream (as shown in the third sketch of fig. 14(b)) the resulting spanwise lift distribution can be obtained from reference 15, but no chordwise distributions are given by this method.

In the case of the first two plan forms shown in figure 14(b), all the lift carried ahead of the hinge line when the whole wing is at an angle of attack is carried at the hinge line when only the control surface is deflected. The control surface itself carries the same lift as it would if the whole wing were deflected.

For wings of low aspect ratio the apparent-mass concept also indicates that the two-dimensional value of α_δ cannot be used; instead a value close to 1 should be used for wings of very low aspect ratio such as those shown in figure 14.

REFERENCES

1. Schrenk, O.: A Simple Approximation Method for Obtaining the Spanwise Lift Distribution. NACA TM 948, 1940.

2. Diederich, Franklin W.: A Simple Approximate Method for Obtaining Spanwise Lift Distributions Over Swept Wings. NACA RM L7I07, 1948.

3. Sivells, James C.: An Improved Approximate Method for Calculating Lift Distributions Due to Twist. NACA TN 2282, 1951.

4. Diederich, Franklin W.: A Plan-Form Parameter for Correlating Certain Aerodynamic Characteristics of Swept Wings. NACA TN 2335, 1951.

5. Diederich, Franklin W.: Approximate Aerodynamic Influence Coefficients for Wings of Arbitrary Plan Form in Subsonic Flow. NACA TN 2092, 1950.

6. Murray, Harry E.: Comparison with Experiment of Several Methods of Predicting the Lift of Wings in Subsonic Compressible Flow. NACA TN 1739, 1948.

7. DeYoung, John, and Harper, Charles W.: Theoretical Symmetric Span Loading at Subsonic Speeds for Wings Having Arbitrary Plan Form. NACA Rep. 921, 1948.

8. Jones, Robert T.: Properties of Low-Aspect-Ratio Pointed Wings at Speeds Below and Above the Speed of Sound. NACA Rep. 835, 1946. (Supersedes NACA TN 1032.)

9. Lomax, Harvard, and Heaslet, Max. A.: Linearized Lifting-Surface Theory for Swept-Back Wings With Slender Plan Forms. NACA TN 1992, 1949.

10. Bird, John D.: Some Theoretical Low-Speed Span Loading Characteristics of Swept Wings in Roll and Sideslip. NACA Rep. 969, 1950. (Supersedes NACA TN 1839.)

11. DeYoung, John: Theoretical Antisymmetric Span Loading for Wings of Arbitrary Plan Form at Subsonic Speeds. NACA TN 2140, 1950.

12. Toll, Thomas A., and Queijo, M. J.: Approximate Relations and Charts for Low-Speed Stability Derivatives of Swept Wings. NACA TN 1581, 1948.

13. Weissinger, J.: The Lift Distribution of Swept-Back Wings. NACA TM 1120, 1947.

14. Falkner, V. M.: The Calculation of Aerodynamic Loading on Surfaces of Any Shape. R. & M. No. 1910, British A.R.C., 1943.

15. Diederich, Franklin W., and Zlotnick, Martin: Theoretical Spanwise Lift Distributions of Low-Aspect-Ratio Wings at Speeds Below and Above the Speed of Sound. NACA TN 1973, 1949.

16. Robinson, A.: Aerofoil Theory for Swallow Tail Wings of Small Aspect Ratio. Rep. No. 41, College of Aero., Cranfield (British), Oct. 1950.

17. Gdaliahu, M.: The Lift Increment of an Aerofoil Due to Variation of Incidence Along the Span, and a Simple Method of Estimating the Lift Distribution. R. & M. No. 2261, British A.R.C., 1945.

18. Diederich, Franklin W.: Calculation of the Aerodynamic Loading of Swept and Unswept Flexible Wings of Arbitrary Stiffness. NACA Rep. 1000, 1951. (Supersedes NACA TN 1876.)

19. Swanson, Robert S., and Crandall, Stewart M.: An Electromagnetic-Analogy Method of Solving Lifting-Surface-Theory Problems. NACA ARR L5D23, 1945.

TABLE 1.- GEOMETRIC CHARACTERISTICS, CONSTANTS, AND LIFT-CURVE SLOPES OF THE SIX PLAN FORMS CONSIDERED IN FIGURE 8

Plan form	A	Λ, deg	λ	F	C_1	C_2	C_3	k_0	C_{L_α}		$\bar{y}^*$	
									Equation 3	Method of reference 13	Equation 9	Method of reference 13
1	6	0	0.5	6.00	0.301	0.441	0.254	0.721	4.529	4.321	0.430	0.425
2	6	45	.5	8.48	.405	.266	.327	.792	3.517	3.444	.448	.455
3	6	45	1.0	8.48	.405	.266	.327	.792	3.517	3.237	.471	.480
4	3	30	1.5	3.46	.184	.652	.163	.577	3.140	2.795	.449	.452
5	3	45	0	4.24	.221	.584	.194	.634	2.817	2.843	.414	.407
6	3	60	.5	6.00	.301	.441	.254	.949	2.265	2.290	.445	.455

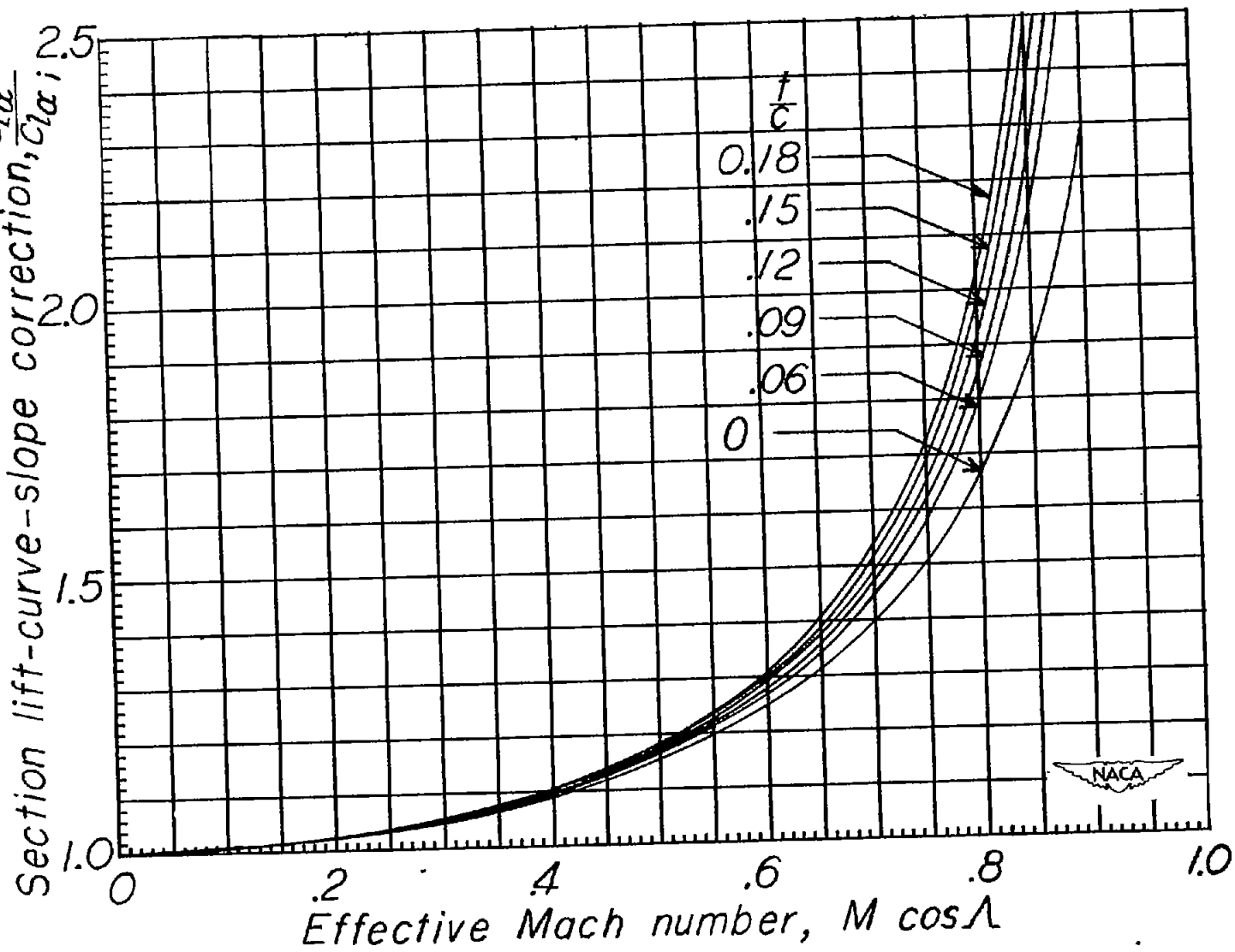

Figure 1.- Section lift-curve-slope correction.

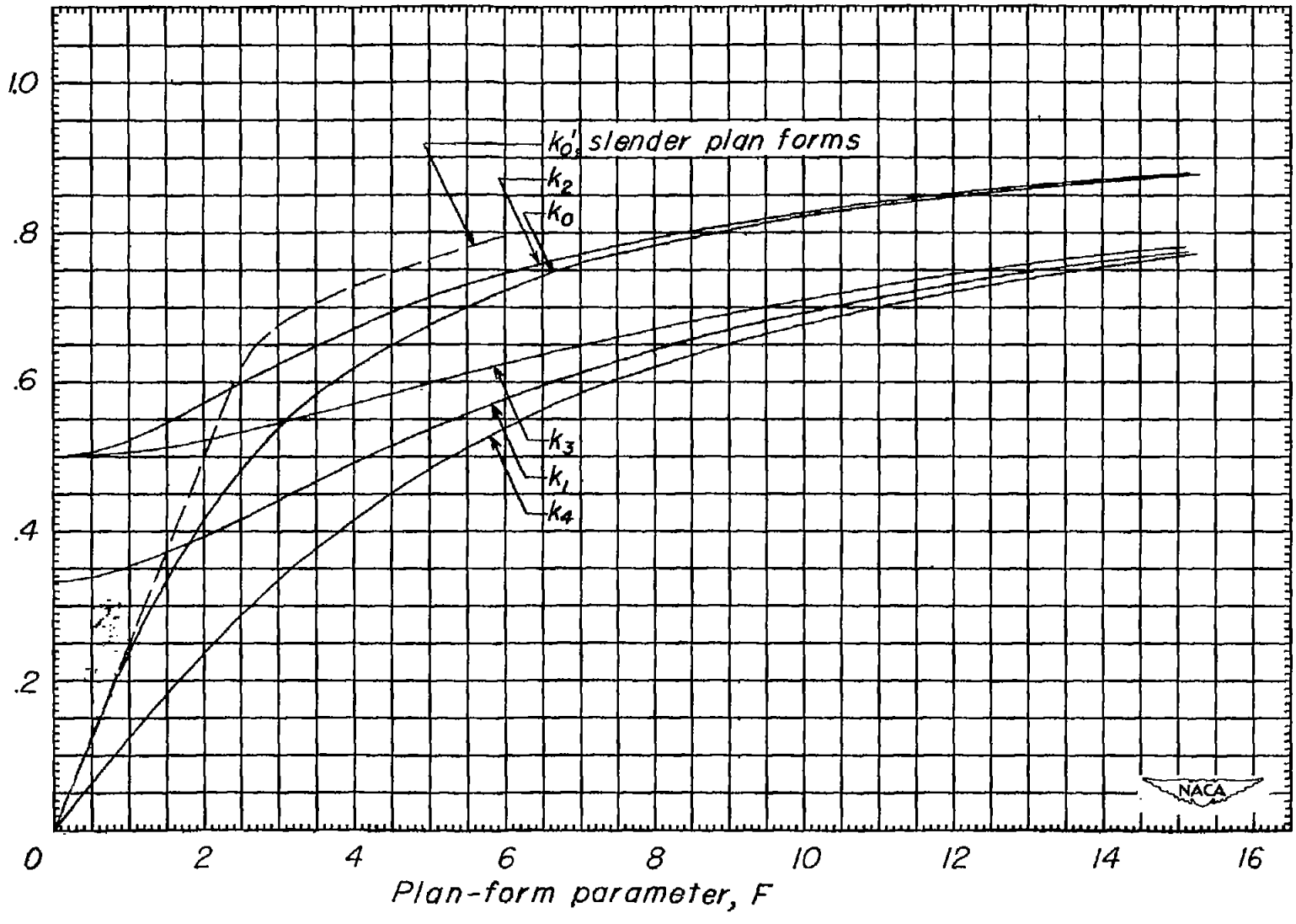

Figure 2.- Factors k_0, k_1, k_2, k_3, and k_4.

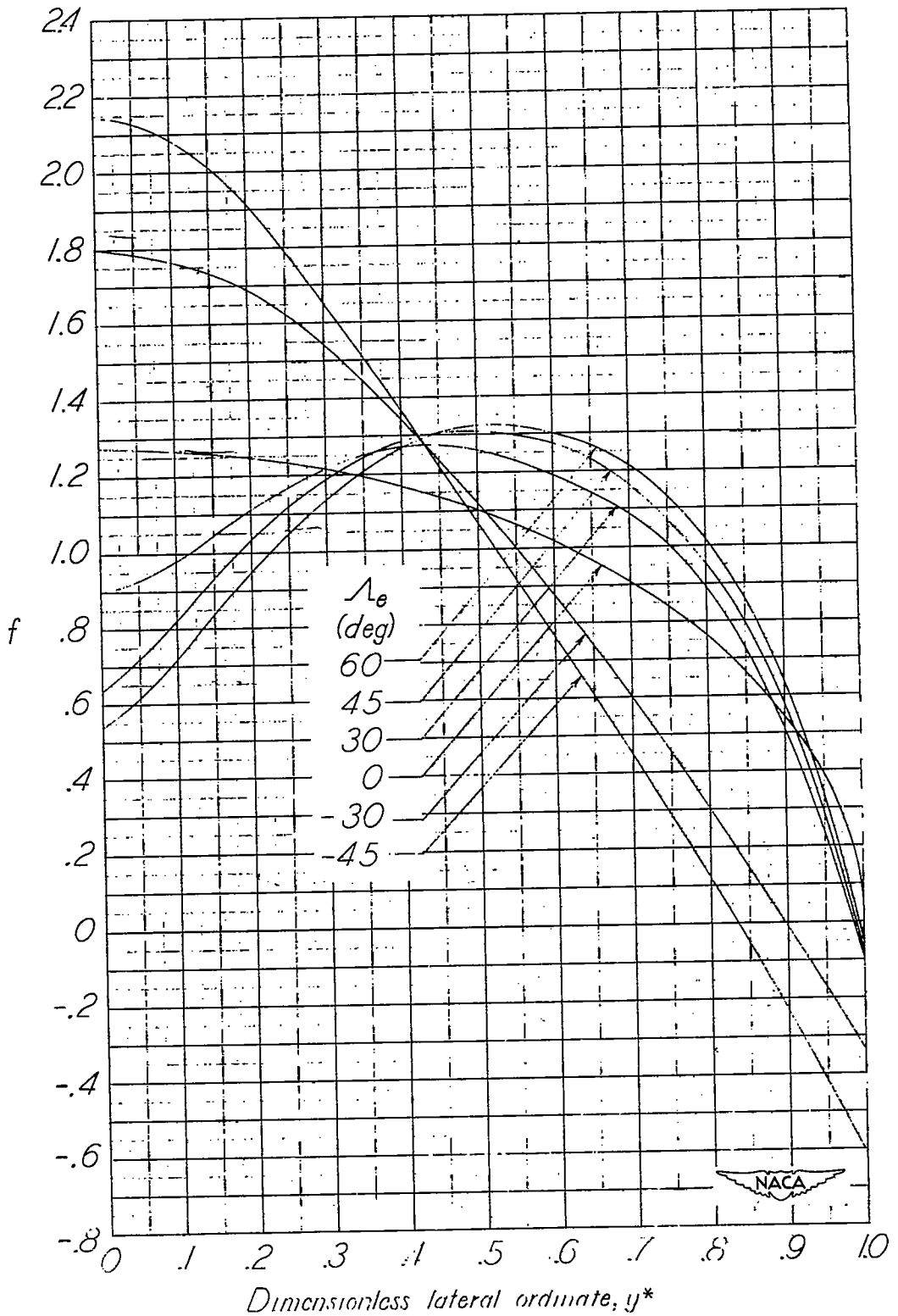

Figure 3.- The lift-distribution function f.

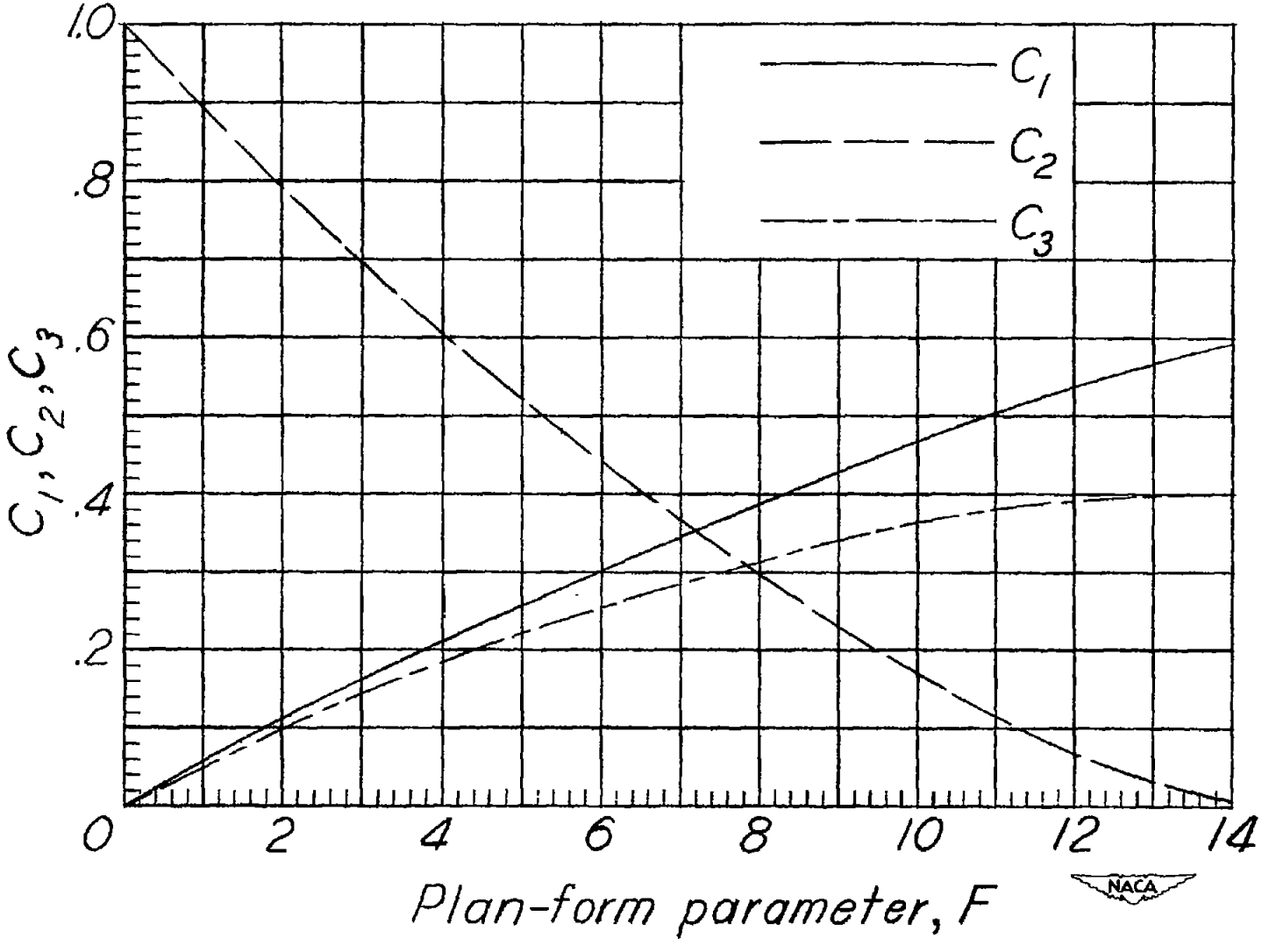

Figure 4.- The lift-distribution constants C_1, C_2, and C_3.

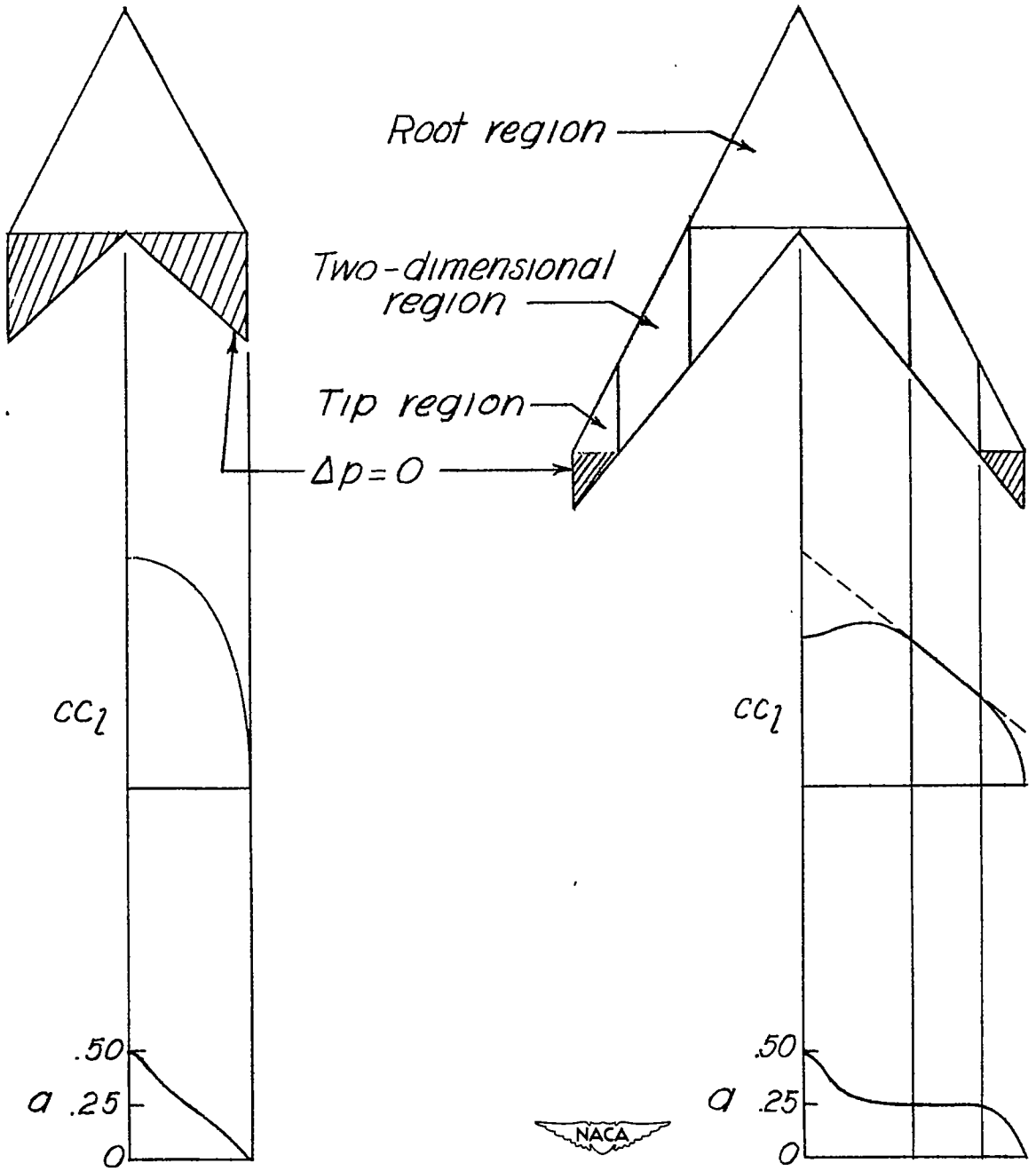

(a) Small plan-form parameter. (b) Large plan-form parameter.

Figure 5.- Approximate lift distributions and section aerodynamic centers on wings with slender plan forms.

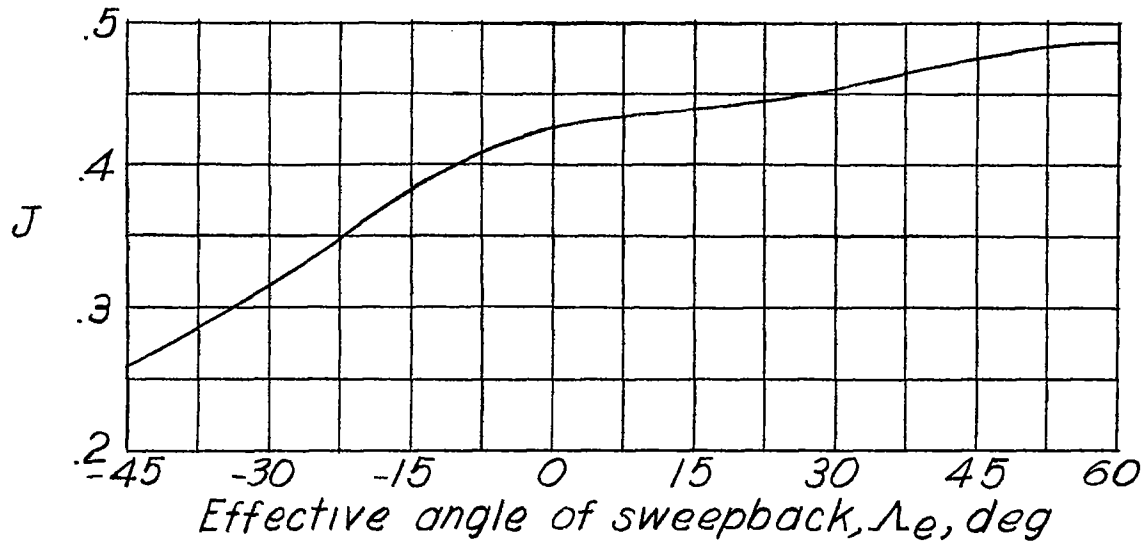

(a) Spanwise center of pressure J.

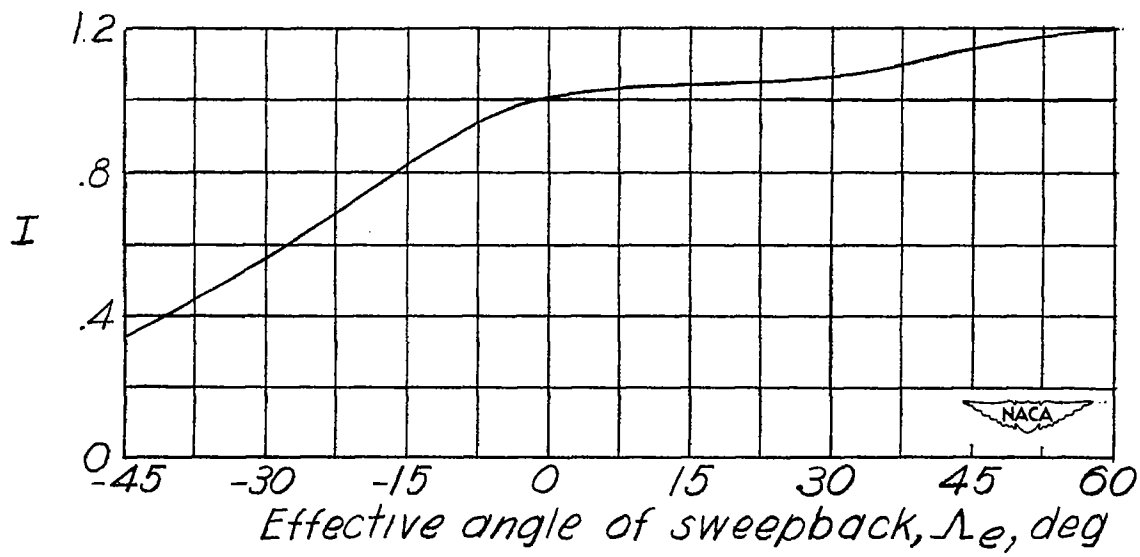

(b) Moment of inertia I.

Figure 6.- Centroid of area and moment of inertia of lift-distribution function f.

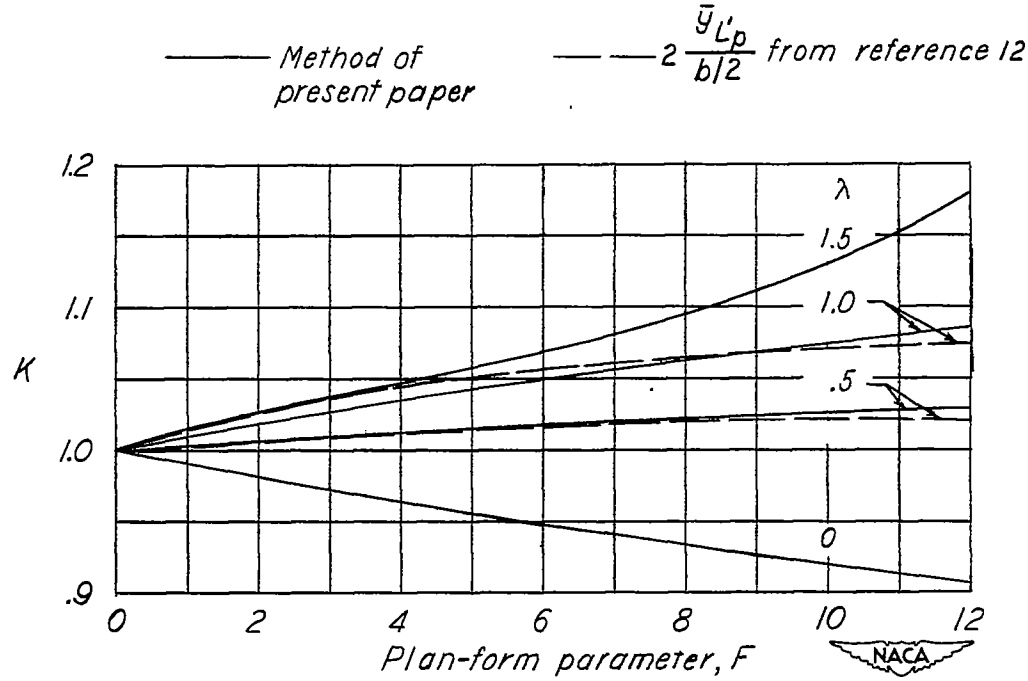

(a) Comparison between the correction factor K and the factor $2\frac{\bar{y}_{L'_p}}{b/2}$.

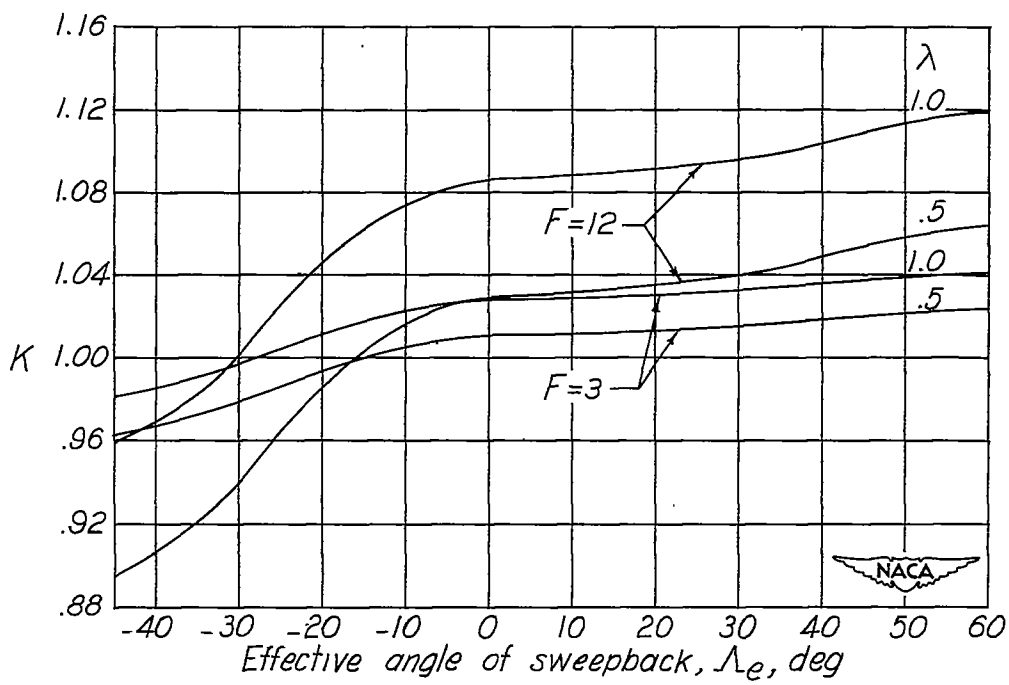

(b) Effect of sweep on the factor K.

Figure 7.- The correction factor K.

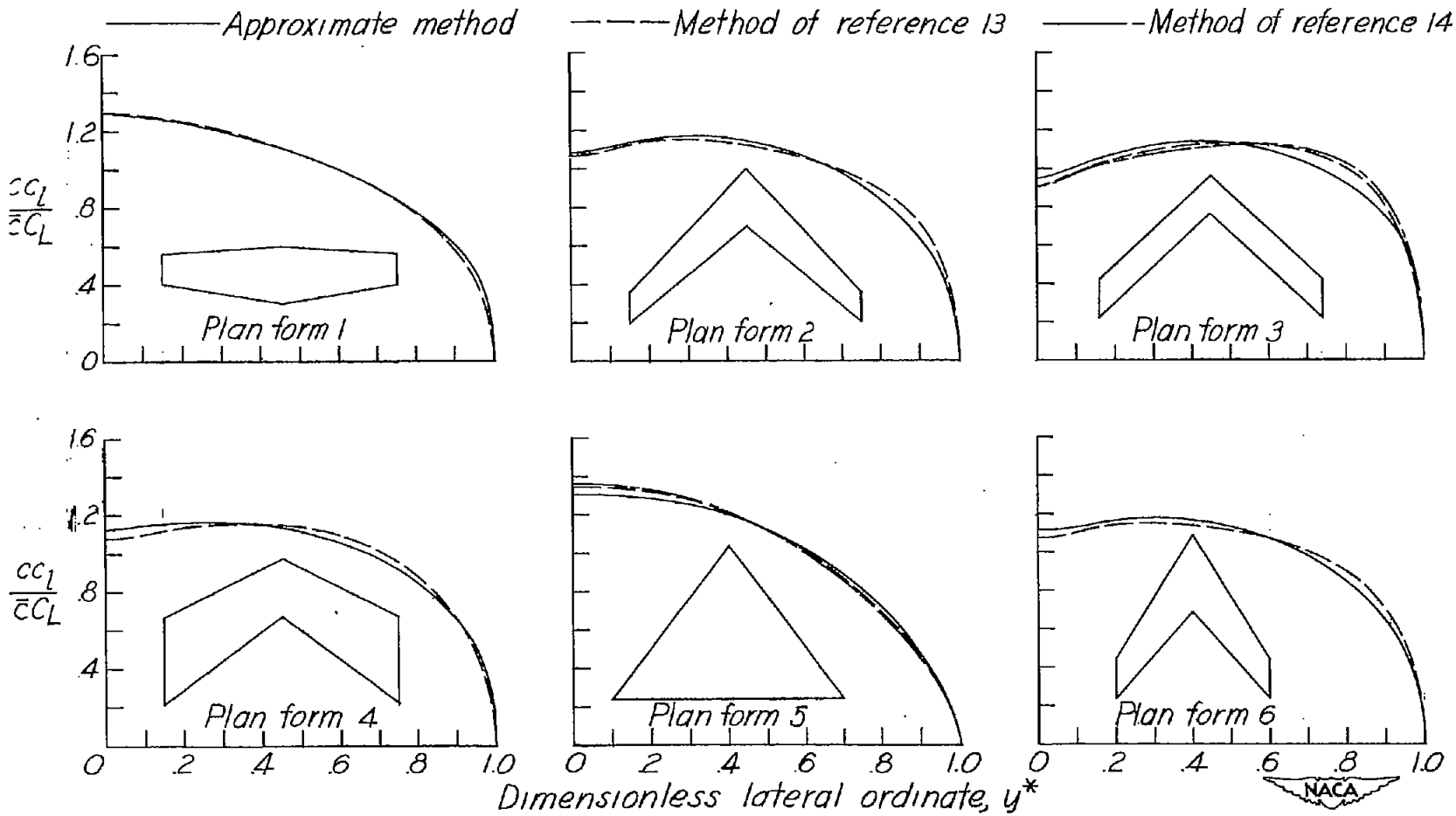

Figure 8.- Additional lift distribution for six plan forms.

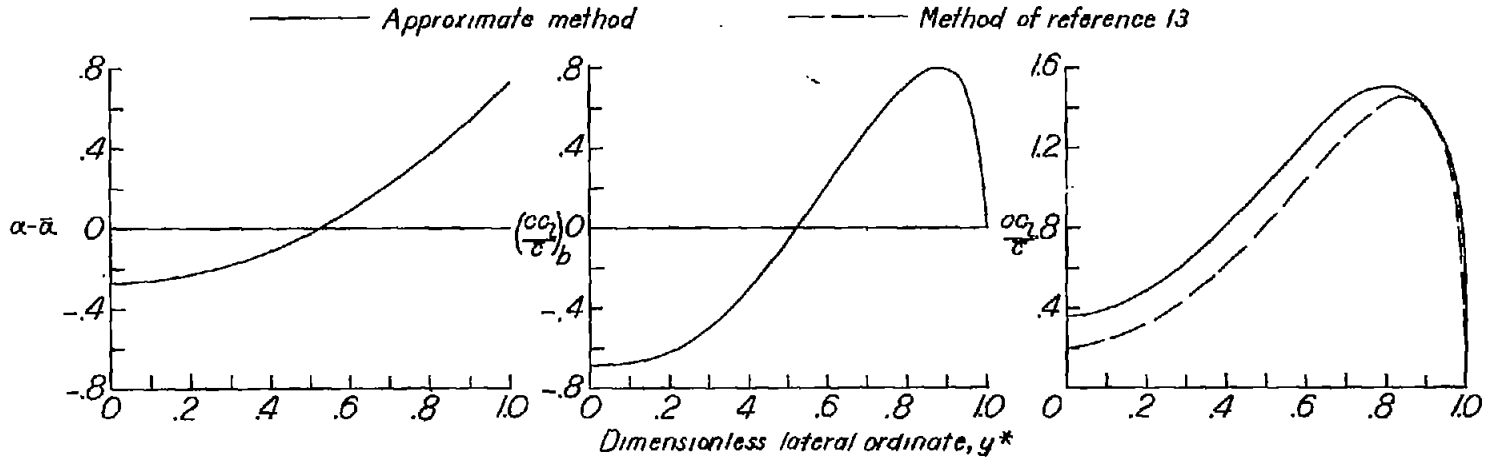

(a) Unit parabolic twist.

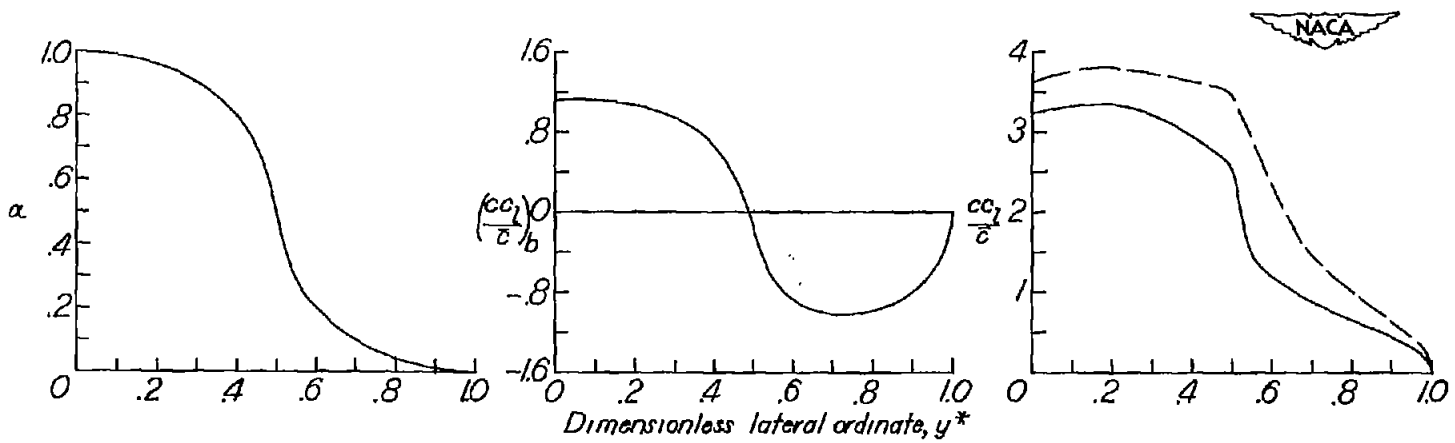

(b) Unit deflection of half-semispan flap.

Figure 9.- Symmetric lift distributions for plan form 2.

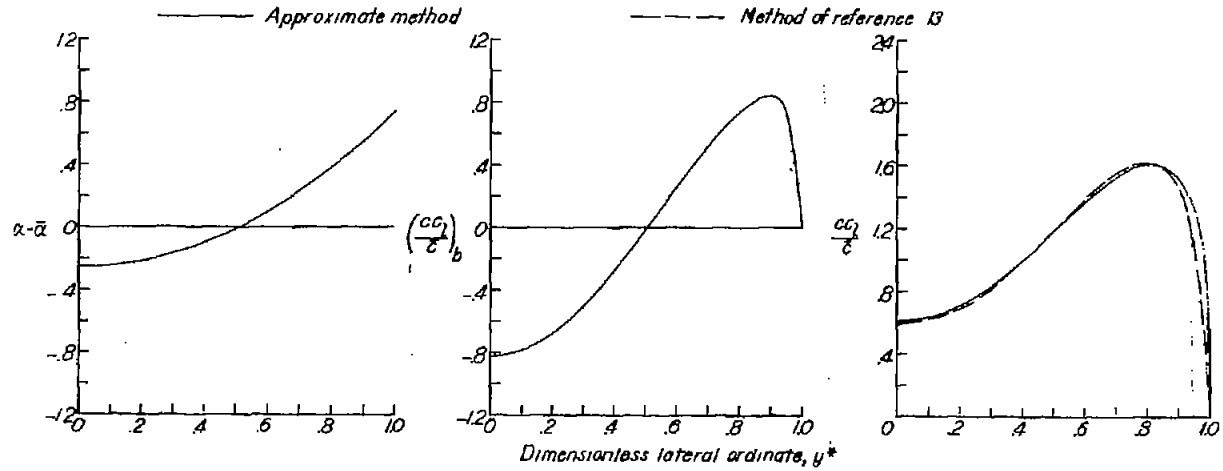

(a) Unit parabolic twist.

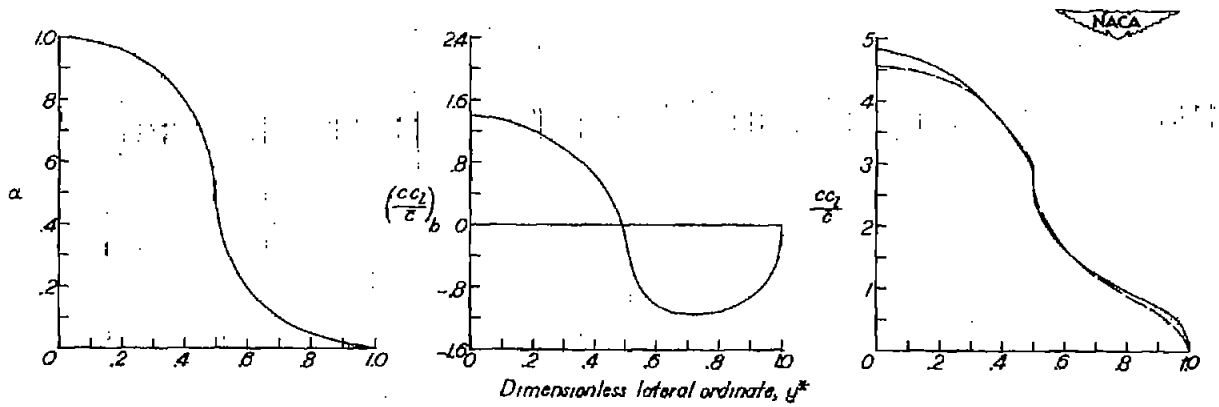

(b) Unit deflection of half-semispan flap.

Figure 10.- Symmetric lift distributions for plan form 1.

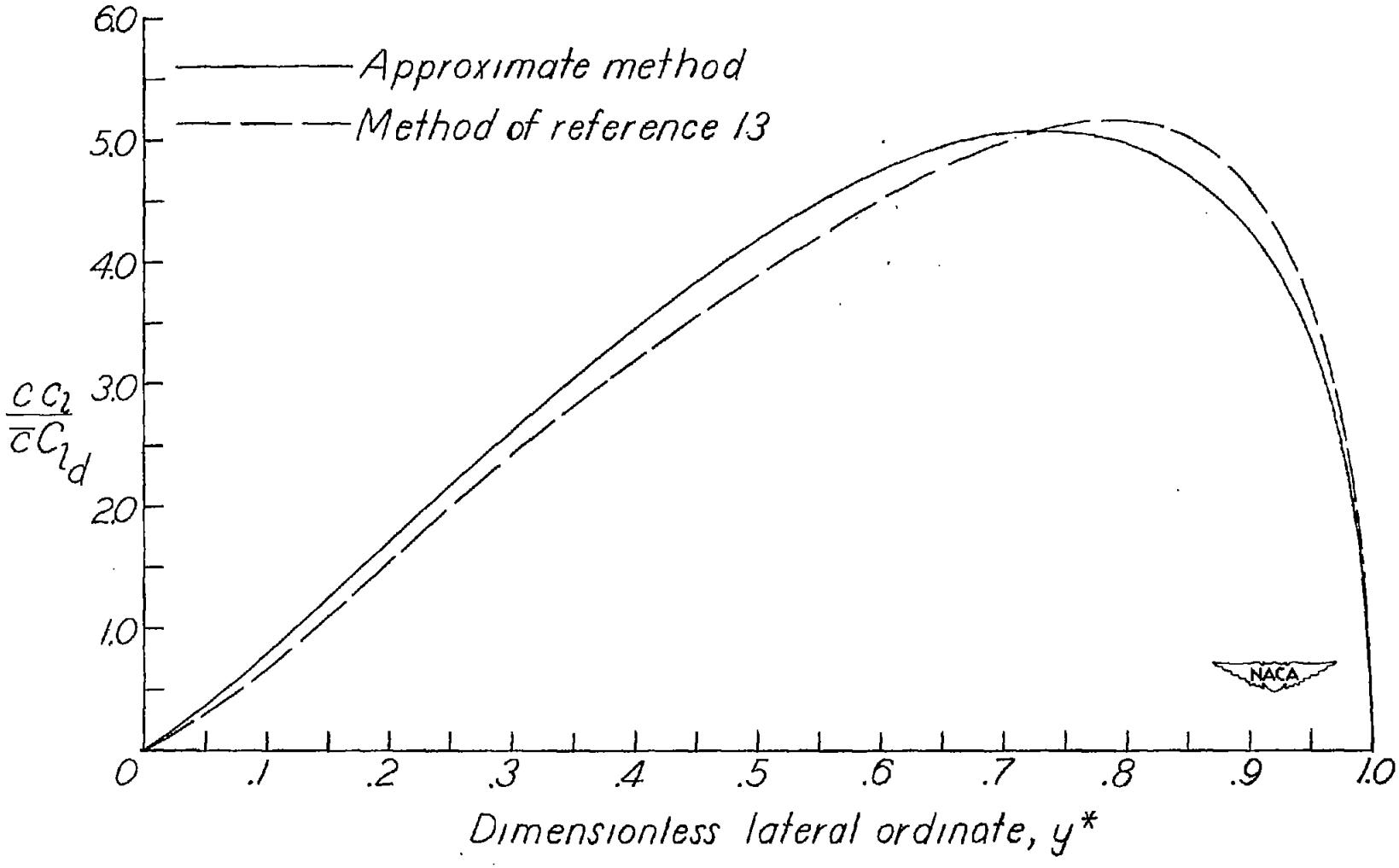

(a) Linear twist (damping-in-roll case).

Figure 11.- Antisymmetric lift distribution for plan form 2.

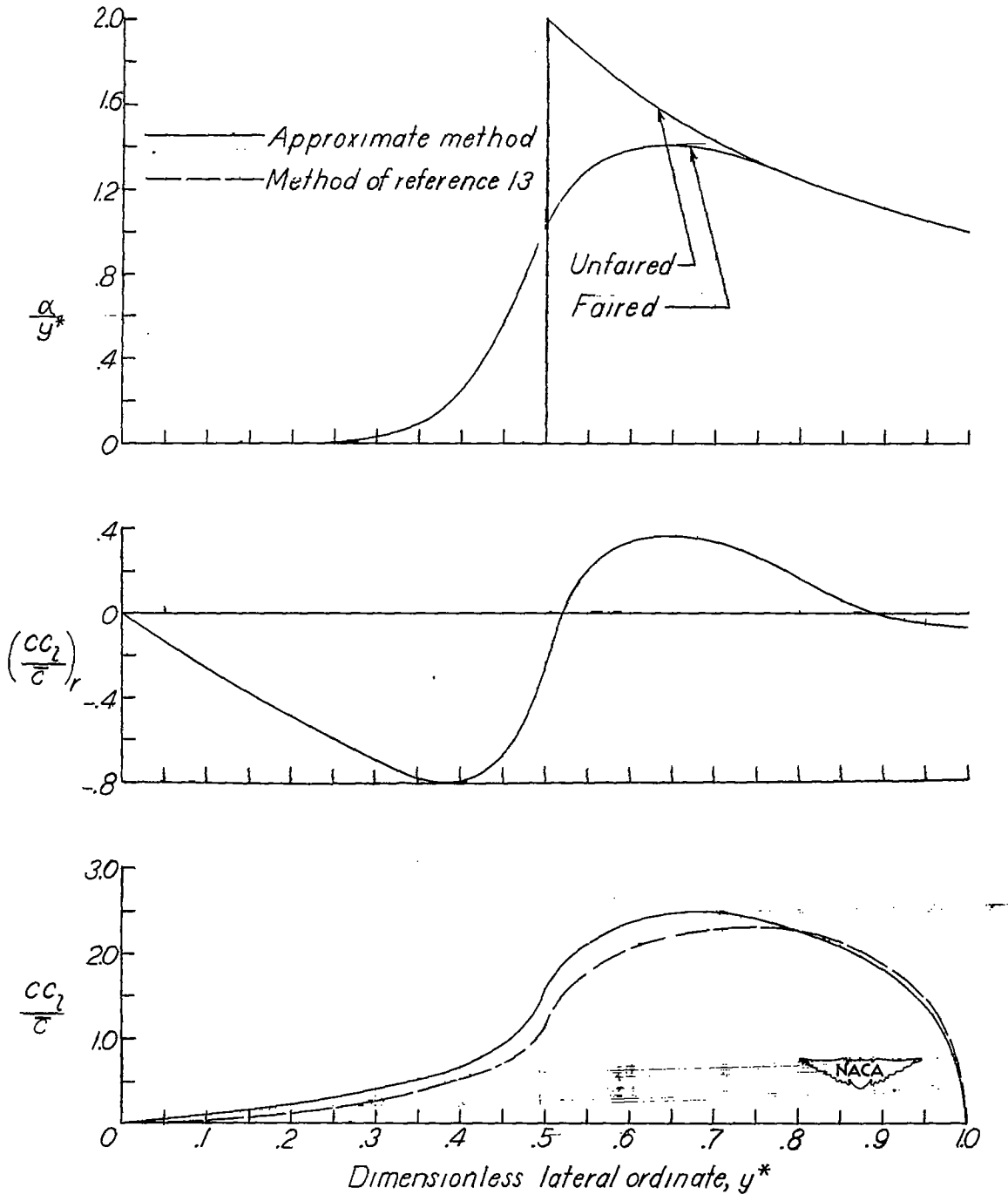

(b) Unit deflection of half-semispan flap.

Figure 11.- Concluded.

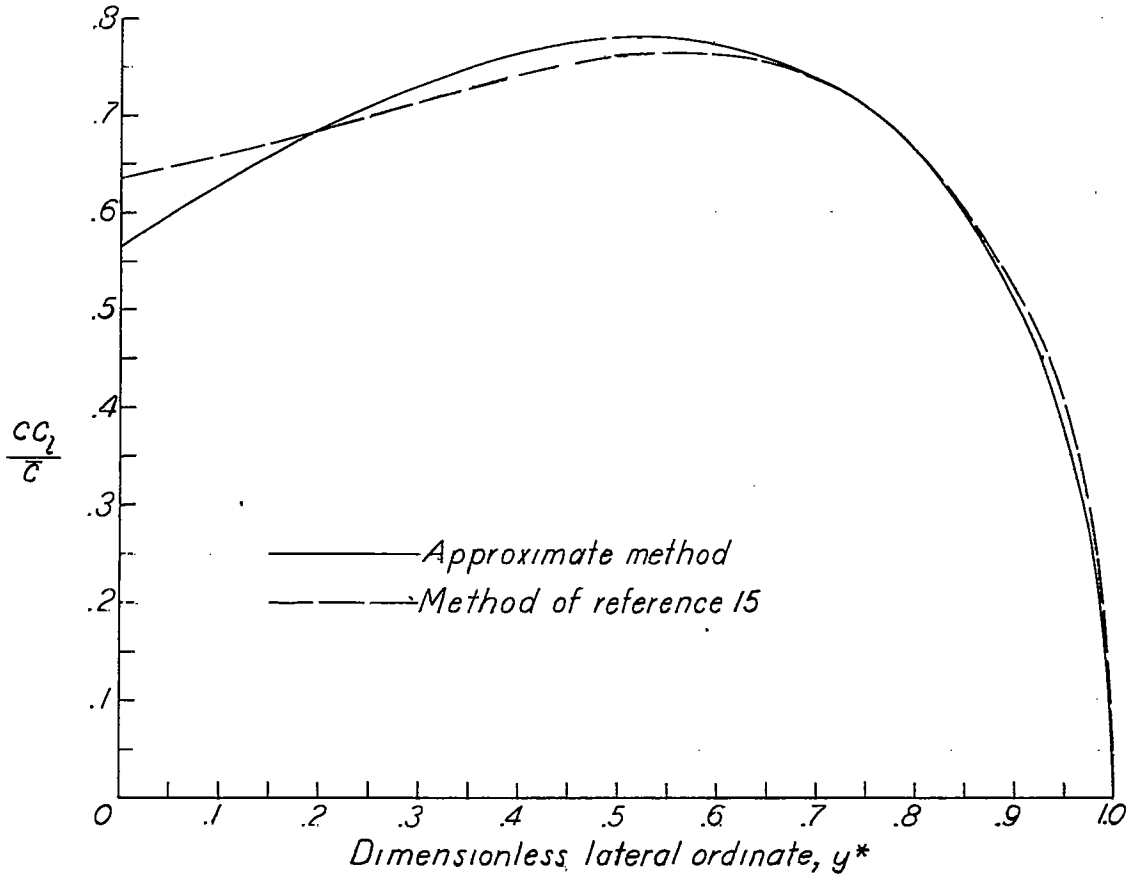

(a) Symmetric linear twist.

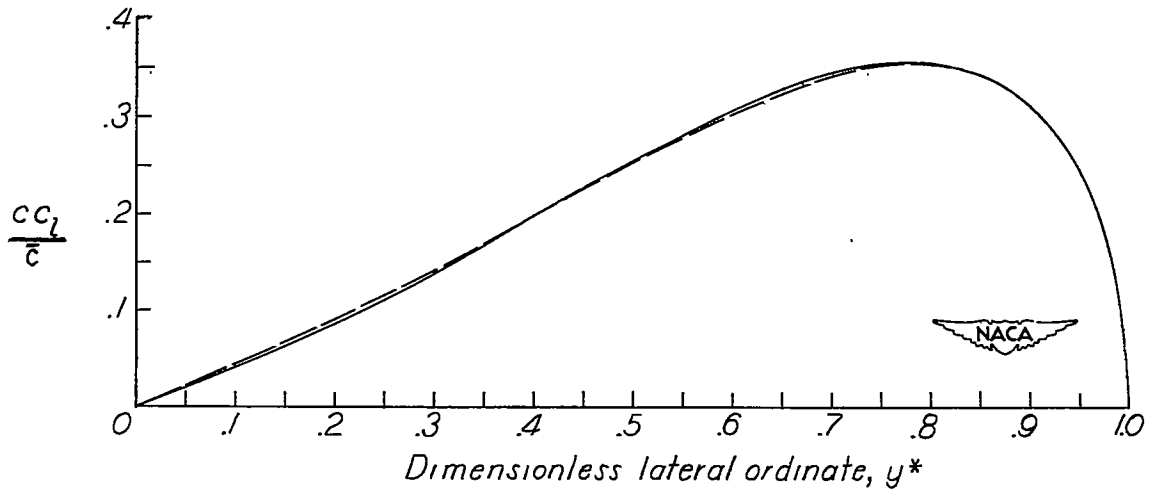

(b) Antisymmetric quadratic twist.

Figure 12.- Lift distributions for wings of very low aspect ratio.

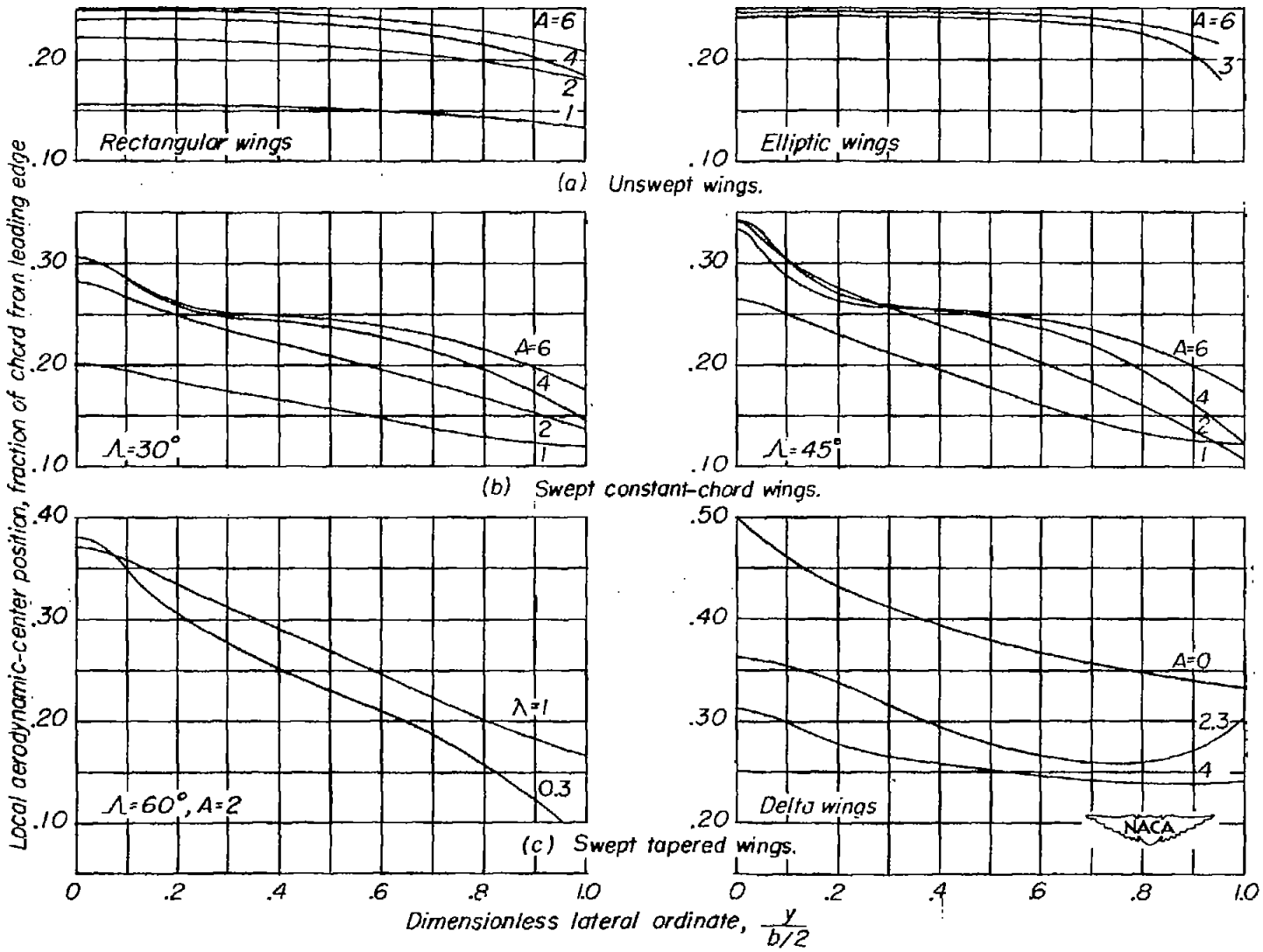

Figure 13.- Local aerodynamic-center positions for various plan forms.

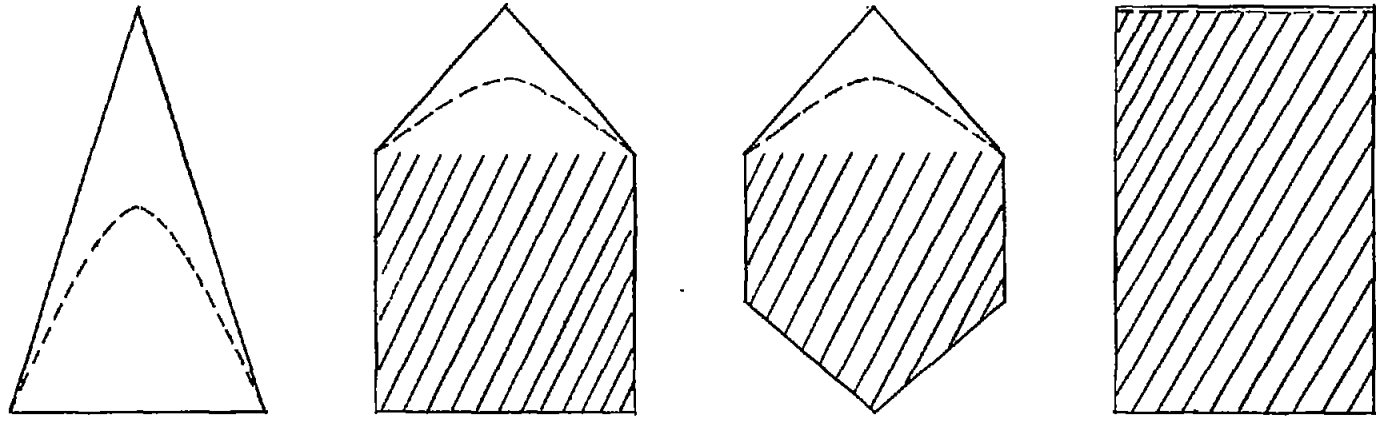

(a) Aerodynamic-center locations.

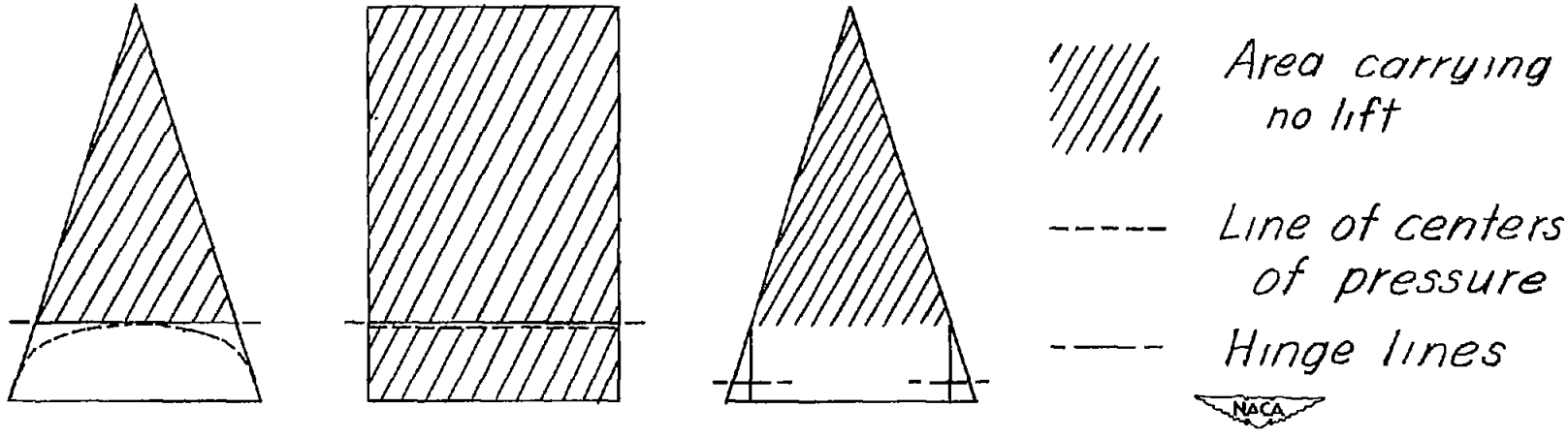

(b) Center-of-pressure locations due to control deflection.

Figure 14.- Aerodynamic-center locations and local centers of pressure due to control deflection on low-aspect-ratio wings without reentrant trailing edges according to low-aspect-ratio theory.